iScience

CellPress

Article

Extracytoplasmic Function σ Factors Can Be Implemented as Robust Heterologous Genetic Switches in *Bacillus subtilis*

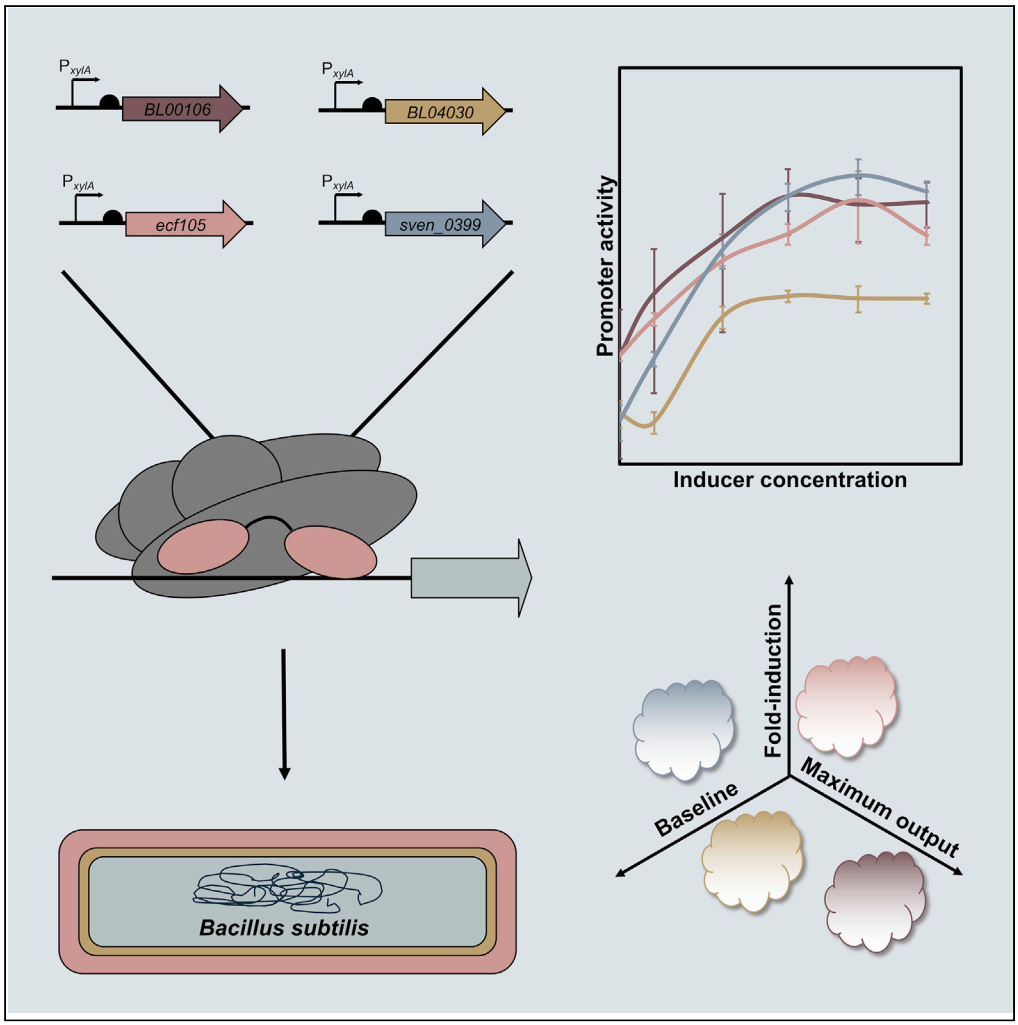

Daniela Pinto, Franziska Dürr, Friederike Froriep, Dayane Araújo, Qiang Liu, Thorsten Mascher

thorsten.mascher@tu-dresden.de

HIGHLIGHTS

Four heterologous ECF-based genetic switches were implemented in *Bacillus subtilis*

Each ECF switch was excessively modified and comprehensively evaluated

The robustness to genetic perturbations differed significantly between switches

B. subtilis has a narrow phylogenetic acceptance range for heterologous ECFs

Pinto et al., iScience *13*, 380–390
March 29, 2019
https://doi.org/10.1016/j.isci.2019.03.001

iScience

CellPress

Article

Extracytoplasmic Function σ Factors Can Be Implemented as Robust Heterologous Genetic Switches in *Bacillus subtilis*

Daniela Pinto,[1] Franziska Dürr,[1] Friederike Froriep,[2] Dayane Araújo,[2] Qiang Liu,[2] and Thorsten Mascher[1,3,*]

SUMMARY

In bacteria, the promoter specificity of RNA polymerase is determined by interchangeable σ subunits. Extracytoplasmic function σ factors (ECFs) form the largest and most diverse family of alternative σ factors, and their suitability for constructing genetic switches and circuits was already demonstrated. However, a systematic study on how genetically determined perturbations affect the behavior of these switches is still lacking, which impairs our ability to predict their behavior in complex circuitry. Here, we implemented four ECF switches in *Bacillus subtilis* and comprehensively characterized their robustness toward genetic perturbations, including changes in copy number, protein stability, or antisense transcription. All switches show characteristic dose-response behavior that varies depending on the individual ECF-promoter pair. Most perturbations had performance costs. Although some general design rules could be derived, a detailed characterization of each ECF switch before implementation is recommended to understand and thereby accommodate its individual behavior.

INTRODUCTION

In bacteria, transcription is mediated by a single DNA-directed RNA polymerase (RNApol). This enzyme is composed of four essential subunits: the α subunit is involved in RNApol assembly and interaction with transcriptional regulators and promoters, the β and β′ subunits form the catalytic core, and the variable σ subunit is required for promoter recognition and transcription initiation (Lane and Darst, 2010a, 2010b). In addition, non-essential subunits also exist, including the ω subunit, which promotes RNApol assembly and is present in all domains of life (El-Gebali et al., 2019; Mathew and Chatterji, 2006), or the Firmicutes-specific δ subunit that decreases RNApol affinity toward DNA and consequently increases specificity (López De Saro et al., 1999).

Because of the central role that transcription initiation plays in determining gene expression and hence protein production in bacteria, regulating the activity of this enzyme has been one of the major points of focus of synthetic biology. So far, the vast majority of approaches have focused on promoter engineering and the use of repressors (Alper et al., 2005; Stanton et al., 2014), and more recently the use of single-subunit RNA polymerases (Meyer et al., 2015). Although these attempts have been very successful and allowed the implementation of numerous regulatory switches and circuits, the number of well-characterized switches is still relatively low thereby limiting the complexity of the resulting genetic circuitry.

The potential of exploiting the RNApol subunits themselves has been mostly neglected. However, the σ subunit, in particular, holds great engineering potential owing to its role in determining the DNA specificity of RNApol via interaction with their target promoters. In addition to the essential primary σ factors in charge of housekeeping functions, bacteria contain a large diversity of non-essential alternative σ factors that control specific subsets of genes. This ability to redirect RNApol is based on alternative promoter signatures specific of each σ factor (Pinto and Mascher, 2016).

The largest and most diverse group of alternative σ factors is the extracytoplasmic function family, currently divided into 94 groups that are supported by sequence similarity, genomic context conservation, and target promoter sequence (Pinto and Mascher, 2016). Extracytoplasmic function σ factors (ECFs) exhibit several attractive features for engineering. (1) They are widespread in bacteria (Staroń et al., 2009); (2) they recognize alternative promoters that are unrelated to those recognized by the housekeeping σ factor (Staroń et al., 2009); (3) they are simple and highly modular by containing only two of the conserved σ factor

[1]Technische Universität Dresden, Institute of Microbiology, Zellescher Weg 20b, 01217 Dresden, Germany

[2]Ludwig-Maximilians-Universität München, Department Biology I, Großhaderner Str. 2-4, 82152 Planegg-Martinsried, Germany

[3]Lead Contact

*Correspondence: thorsten.mascher@tu-dresden.de

https://doi.org/10.1016/j.isci.2019.03.001

domains, each interacting with one of the key promoter elements (i.e., −35 and −10 elements) (Feklístov et al., 2014); and (4) the activity of ECFs is naturally controlled by a variety of mechanisms (Mascher, 2013) that can potentially also be engineered. This implies that, at least theoretically, ECF circuits implemented in one organism can be easily transferred to another given that all bacteria have σ factor-dependent transcriptional initiation. In addition, their small size and reduced number of conserved domains makes them easy to manipulate.

Despite these attractive features, surprisingly few attempts have so far been made to implement σ-dependent regulatory switches and circuits (Annunziata et al., 2017; Bervoets et al., 2018; Chen and Arkin, 2012; Pinto et al., 2018; Rhodius et al., 2013; Shin and Noireaux, 2012). However, these studies have already established that σ factors can indeed be used to build heterologous switches and circuits in *Escherichia coli*, *Bacillus subtilis,* and cell-free systems. Moreover, by taking advantage of the modularity of ECFs, combinatorial synthesis can be used to increase the diversity of ECF-based switches.

Despite these promising results, the robustness of ECF switches has never been evaluated in detail, thereby preventing their widespread use (e.g., for the assembly of more complex circuits). Here, we have implemented ECF switches in the Gram-positive model organism *B. subtilis* and comprehensively assessed their behavior by analyzing their responses to changes in copy number, different inducible promoters, variation in the length of their target promoters, ECF stability, and the effect of antisense transcription. We demonstrate that *B. subtilis* has a significantly narrower phylogenetic range of acceptance of heterologous σ factors, in contrast to *E. coli* (Rhodius et al., 2013). In addition, the individual ECF switches do not respond identically when subjected to genetic perturbations. Our analysis highlights the need to expand the characterization of any ECF switch beyond their characteristic dose-response curve. Moreover, it uncovers the factors that might influence ECF switch behavior and underscores the critical importance of carefully designing ECF-based genetic circuits.

RESULTS

ECF Switches from Different Origins

ECFs suitable for implementation in *B. subtilis* had to obey the following rules: (1) they had to belong to ECF groups different from those already encoded in the genome of *B. subtilis* 168 to avoid cross-activation of the ECF target promoter and (2) their target promoter sequence needed to have been either experimentally determined (as is the case of ECF121 of *S. venezuelae;* Bibb et al., 2012) or predicted by comparative genomics in the course of the ECF classification (Pinto and Mascher, 2016). We selected model organisms from the γ-Proteobacteria, α-Proteobacteria, Actinobacteria, and Firmicutes to cover a wide phylogenetic range and thereby increase the diversity of ECFs to be implemented. The ECF profiles of *B. subtilis* 168, *Bacillus licheniformis* ATCC 14580, *Bacillus cereus* ATCC 10987, *E. coli* K-12 DH10β, *Sinorhizobium meliloti* 1021, and *Streptomyces venezuelae* ATCC 10712 were determined and the suitable ECFs selected (Figure 1A).

The ECF switches were implemented following the general design depicted in Figure 1B: transcription of the ECF-encoding gene was controlled by the xylose-inducible P_{xylA} promoter. The ECF genes from *S. meliloti* and *S. venezuelae* were codon adjusted for expression in *B. subtilis* and an N-terminal FLAG tag was added, which is known not to interfere with ECF activity (Dufour et al., 2012; Gangaiah et al., 2014; Mao et al., 2013; Toyoda et al., 2015; Wecke et al., 2012). The corresponding ECF target promoter was inserted upstream of the *luxABCDE* operon of *Photorhabdus luminescens* optimized for *B. subtilis* translation machinery (Schmalisch et al., 2010), thereby allowing to monitor promoter activities based on bioluminescence. Both transcriptional units were inserted into the chromosome at two different well-established loci, hence ensuring a copy number that reflects that of the chromosome: the ECF transcriptional unit was integrated into the *lacA* locus, which encodes a non-essential β-galactosidase involved in galactan utilization (Shipkowski and Brenchley, 2006), whereas the promoter or reporter cassette was integrated into the *sacA* locus, which encodes a non-essential phosphosucrase involved in sucrose utilization (Lepesant et al., 1974). Both loci are located in close vicinity to the chromosomal origin of replication, thereby minimizing any negative positioning effects and ensuring a balanced expression of both transcriptional units (Sauer et al., 2016).

A total of 46 heterologous ECF switches, derived from *S. venezuelae* (33), *S. meliloti* (8), *E. coli* (2), *B. licheniformis* (2), and *B. cereus* (1), were implemented. Four of these switches were active (Figure 1C), whereas the

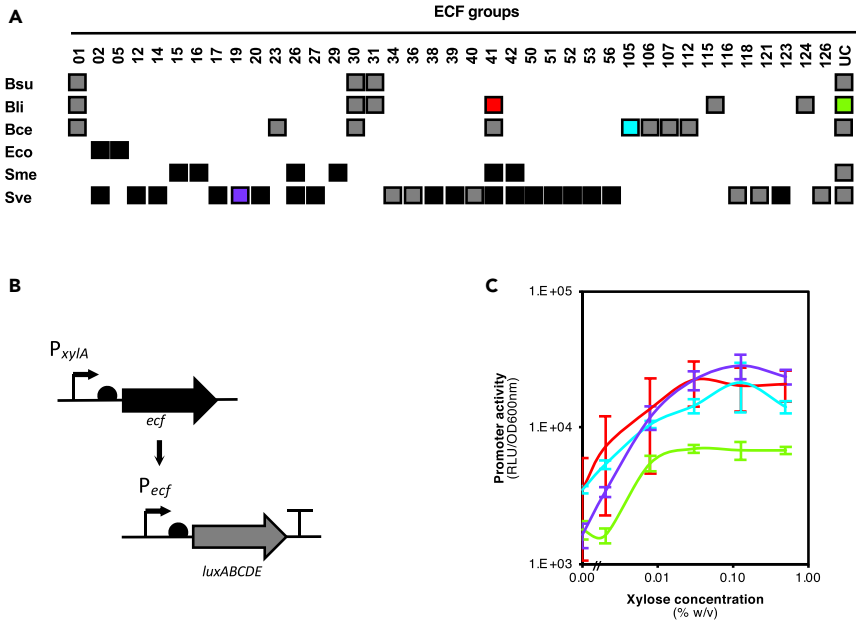

Figure 1. Choice of ECF Switches from Different Origins for Implementation in *B. Subtilis*

(A) The ECF profiles of *B. subtilis* 168 (Bsu), *B. licheniformis* ATCC 14580 (Bli), *B. cereus* ATCC 10987 (Bce), *E. coli* K-12 DH10β (Eco), *S. meliloti* 1021 (Sme), and *S. venezuelae* ATCC 10712 (Sve) are represented. Boxes indicate that ECFs of the group indicated on top are present in the strain indicated on the left. The boxes are colored in black when ECF of that group and organism were tested in B. subtilis 168 and in gray when not tested. The ones shown in (C) are colored accordingly. Forty six ECFs were tested: *B. licheniformis* ATCC 14580 ECF41_BL00106 and ECFUC_BL04030; *B. cereus* environmental isolate ECF105_ecf105; *E. coli* K-12 DH10β ECF02_ECDH10B_2741 and ECF05_ ECDH10B_4491; *S. meliloti* 1021 ECF15_SMb21484 ECF16_SM_b20531, ECF26_SMa0143, ECF26_SMc02713, ECF26_SMc04051, ECF29_SMb20592, ECF41_SM_b20030, and ECF42_SMc01150; and *S. venezuelae* ATCC 10712 ECF02_SVEN_4513, ECF12_SVEN_4870, ECF14_SVEN_4793, ECF17_SVEN_0063, ECF19_SVEN_0399, ECF20_SVEN_6501, ECF27_SVEN_3669, ECF38_SVEN_2914, ECF38_SVEN_3369, ECF38_SVEN_6611, ECF39_SVEN_3215, ECF39_SVEN_3278, ECF39_SVEN_3293, ECF39_SVEN_3759, ECF39_SVEN_4575, ECF41_SVEN_0136, ECF41_SVEN_0858, ECF41_SVEN_3295, ECF41_SVEN_3475, ECF41_SVEN_3480, ECF41_SVEN_3821, ECF41_SVEN_3859, ECF41_SVEN_1176, ECF42_SVEN_4377, ECF42_SVEN_7131, ECF50_SVEN_0980, ECF51_SVEN_0015, ECF52_SVEN_3871, ECF53_SVEN_0434, ECF53_SVEN_6745, ECF56_SVEN_4562, ECF121_SVEN_3185, and ECF123_SVEN_4540.

(B) Generic genetic layout of the ECF switch. Thick arrows represent open reading frames. "T" represents terminators. Half circles represent ribosome-binding sites. Thin arrows represent promoters.

(C) Dose-response curves drawn using the luminescence output value, represented through relative luminescence units (RLU) normalized by the optical density measured at 600 nm (OD600 nm), achieved 90 min after the addition of the inducer to the exponentially growing culture. ECF switches were built using ECFs BL00106 (red), BL04030 (green), ECF105 (blue), and SVEN_0399 (purple). Final concentrations of xylose used for induction of P_{xylA} were 0, 0.002, 0.008, 0.03, 0.125, or 0.5% (w/v). Vertical bars represent standard deviations calculated from three independent experiments.

remaining 42 did not show any activity (Figure S3). None of these switches caused any detectable growth defects (Figure S6), indicating that under these conditions they are not toxic to the host cells.

The active switches were derived from BL00106 (ECF41) and BL04030 (unclassified) ECFs of *B. licheniformis*, ECF105 (ECF105) of *B. cereus*, and SVEN_0399 (ECF19) of *S. venezuelae* and behaved differently (Figure 1C): the BL04030- and ECF105-derived switches have a maximal fold-induction of four, whereas the BL00106 and SVEN_0399 switches have a maximal fold-induction of 6 and 14, respectively. The uninduced baseline activity of these four switches (OFF state) also varied, with BL00106 showing higher variation, whereas the ECF105-dependent switch showing the highest baseline. With regard to the ON state, BL04030 switch showed the lowest, whereas SVEN_0399 had the highest maximal output of the switches. The switching threshold (i.e., the concentration of inducer at which the switch turns ON) was determined to be between 0.002% and 0.008% xylose for BL04030, whereas for the remaining switches, it was observed below 0.002% xylose. Remarkably, three of the four switches behave analogously, that is, their output

gradually increases over a range of inducer concentrations. In contrast, the BL04030 switch behaves in a digital fashion, i.e., there is a threshold concentration at which the switch directly shifts from the OFF to the fully induced state.

The variation in switch behavior already in this simple design suggests different properties when faced with additional phenotypic or genetic constraints. We therefore decided to challenge these four switches by imposing changes in the copy number of each transcriptional unit, the nature of the inducible promoter driving ECF expression, ECF stability, size of the ECF target promoter, and strength of antisense transcription.

Variations in Copy Number of Each Transcriptional Unit

Initially, the copy number of each of the two transcriptional units was changed either separately or simultaneously. Three variants were analyzed for each ECF switch, in which each or both of the constituent transcriptional units were maintained in a multi-copy plasmid. Again, no growth defects were detected on strains carrying these switches (Figure S7).

Whenever both transcriptional units are present in single or multiple copies, both the maximal output and the baseline increased, with an overall pronounced loss of dynamic range (Figure 2; black X versus blue closed circle). A subsequent analysis of strains in which only one of the transcriptional units is present in multiple copies demonstrates that the increase in baseline and the resulting loss of dynamic range is mostly due to the increase in copy number of the promoter or reporter cassette (Figure 2; red closed circle versus green closed circle).

We have further investigated this behavior in the BL00106 switch by testing (1) the influence of *B. subtilis* native ECFs, (2) different plasmid backbones, (3) the existence of other promoter sequences in the BL00106 target promoter (P_{ydfG}) fragment, (4) different orientations of the transcriptional unit, and (5) deficient termination from the transcriptional unit located upstream of P_{ydfG}. The introduction of an array of terminators upstream of the P_{ydfG} promoter significantly decreased the baseline, suggesting that inefficient termination from upstream transcriptional units increased the background signal (Figure S5).

Increasing only the copy number of the ECF-coding gene results in an increased baseline for BL04030, ECF105, and SVEN_0399 and an overall decrease in activity for BL00106 (Figure 2; closed red circle). For BL04030, this change also led to a loss of the digital behavior observed for the single copy switch (Figure S7).

Type of Inducible Promoter Driving ECF Expression

Next, we investigated the behavior of the switches when expression of the ECF is controlled by two different promoters: the xylose-inducible P_{xylA} with an additional copy of the gene coding for its repressor (*xylR*) under the control of its native promoter (P_{xylR}) and the bacitracin-inducible P_{liaI} (Mascher et al., 2004; Radeck et al., 2013; Toymentseva et al., 2012).

The *xyl* operon is present in the genome of *B. subtilis* 168. In the presence of our switches, the repressor XylR has two binding sites: one on the native P_{xylA} promoter and another on the P_{xylA} introduced with our switches. As it has been shown previously that the presence of multiple copies of the XylR operator negatively affects the repression mediated by XylR at its target promoter (Gärtner et al., 1988), we hypothesized that the additional copy of *xylR* could reduce the baseline. However, after implementing the new design to our switches, we instead observed a reduced output if the *xylR*-P_{xylA} cassette was used (Figure 2; red open circle). We hypothesize that this reduction might be caused by the increased amount of XylR, given that in the presence of glucose XylR is known to mediate xylose-independent, glucose-dependent repression of P_{xylA} (Kraus et al., 1994).

The use of P_{liaI} as inducible promoter increased the fold-induction for all switches (Figure 2; blue open circle). In addition, the dose-response curves of the switches change and adopt the characteristic sigmoid shape of P_{liaI}-controlled reporter cassette (Figures S4 and S8). In fact, the shape of the dose-response curve of all ECF switches reflects that of the inducible promoter driving the ECF expression (Figure S4), but with an overall reduced maximal output when compared with the inducible promoters themselves (Figures S4

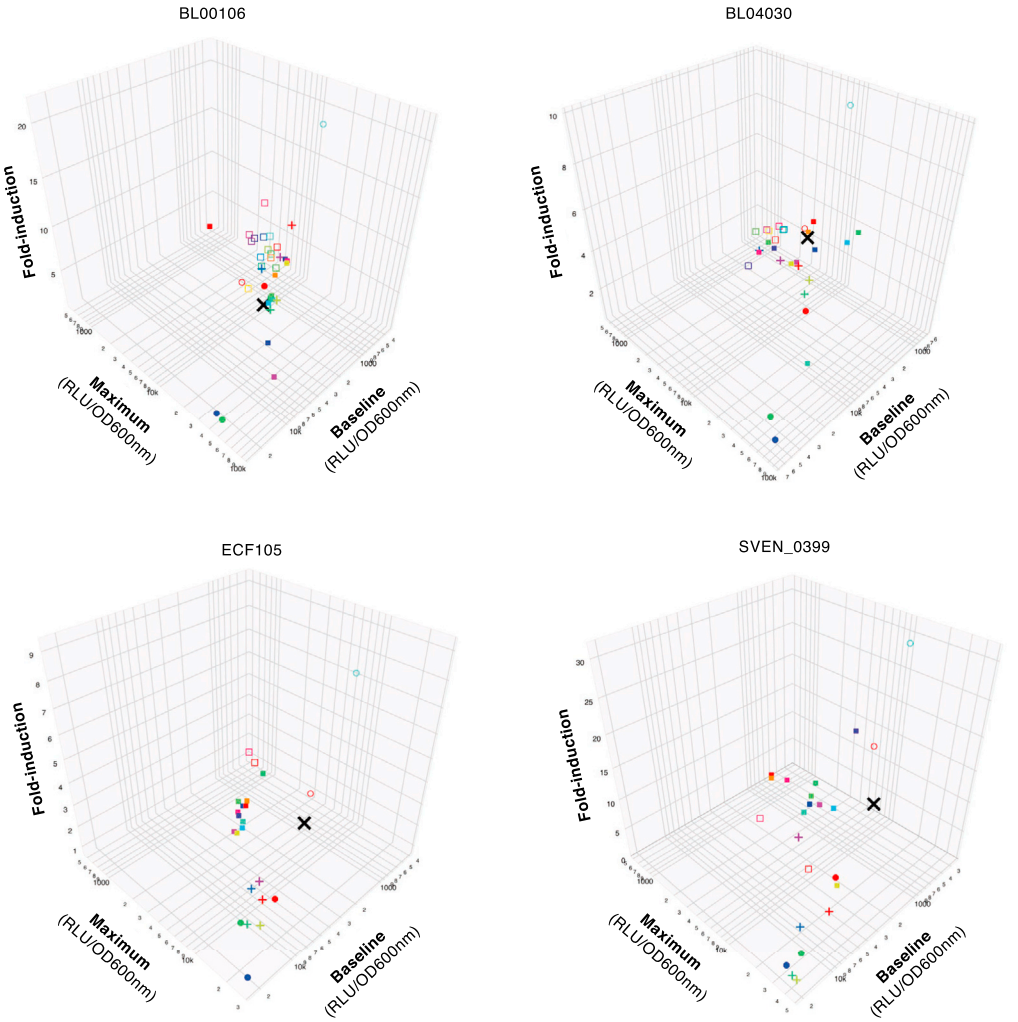

X default switch (as in Figure 1)

● ECF transcriptional unit in plasmid
● reporter transcriptional unit in plasmid
● both transcriptional units in plasmids

○ *xylR*-P_{xylA} inducible promoter
○ P_{lial} inducible promoter

✚ antisense P_{J23101}
✚ antisense P_{liaG}
✚ antisense P_{lepA}
✚ antisense P_{sigW}
✚ antisense P_{veg}

■ LAA ssrA-tag
■ LVA ssrA-tag
■ LDD ssrA-tag
■ LAD ssrA-tag
■ ISV ssrA-tag
■ ISS ssrA-tag
■ HHA ssrA-tag
■ DVS ssrA-tag
■ DAG ssrA-tag
■ ASV ssrA-tag
■ AAV ssrA-tag

□ P_{ydfG}-122 to +30 / $P_{BL04030}$-51 to +8 / P_{ECF105}-50 to +1 / P_{SVEN_0399}-35 to +1
□ P_{ydfG}-122 to +17
□ P_{ydfG}-122 to +10 / $P_{BL04030}$-36 to +8
□ P_{ydfG}-122 to +1
□ P_{ydfG}-56 to +78 / $P_{BL04030}$-21 to +8
□ P_{ydfG}-56 to +30
□ P_{ydfG}-56 to +17 / $P_{BL04030}$-66 to +8
□ P_{ydfG}-56 to +10
□ P_{ydfG}-56 to +1 / $P_{BL04030}$-66 to -23
□ P_{ydfG}-35 to +78
□ P_{ydfG}-35 to +30 / $P_{BL04030}$-66 to -38
□ P_{ydfG}-35 to +17
□ P_{ydfG}-35 to +10 / $P_{BL04030}$-51 to +8
□ P_{ydfG}-35 to +1 / $P_{BL04030}$-36 to -8 / P_{ECF105}-30 to +1 / P_{SVEN_0399}-129 to +71

Figure 2. Robustness of Heterologous ECF Switches in *B. subtilis*

The four three-dimensional scatterplots show the behavior of the ECF switches upon the imposed alterations. Each plot corresponds to one ECF: BL00106 and BL04030 of *B. licheniformis*, ECF105 of *B. cereus*, and SVEN_0399 of *S. venezuelae*. The x axis corresponds to the baseline value of the switch; the y axis corresponds to the maximum output level of the switch, and the z axis corresponds to the maximal fold-induction. Baseline refers to the output observed in the absence of inducer, maximal output refers to the output value upon induction with the maximal concentration of inducer, and fold-induction refers to the ratio between maximal output and baseline values. Baseline and maximal output level are shown as relative luminescence units (RLU) normalized by the optical density at 600 nm (OD600 nm). All data points represent

Figure 2. *Continued*

averages of three independent experiments in which cells were grown to exponential phase, the expression of the ECF was induced by 0.5% xylose (or 10 μg/mL of bacitracin for P_{lial}-driven switches), and the values used were obtained 90 min after induction. The legend at the bottom of the figure shows the correspondence between the symbols and the performed alterations.

and S8). This reduction is most likely due to the fact that the inducible and ECF target promoters are functionally connected and the output of one promoter (inducible promoter) corresponds to the input of the other (ECF target promoter) (Nielsen et al., 2016; Pinto et al., 2018).

Changing the Stability of the ECF

Translation is a crucial cellular process and is constantly monitored to recognize and release, e.g., stalled ribosomes. Many bacterial species target the resulting truncated proteins for degradation by the co-translational addition of the SsrA-tag, a small peptide encoded in the *ssrA* transfer-messenger RNA. Tagged proteins are then recognized and degraded by cytoplasmic proteases (Karzai et al., 2000). This mechanism, which has been studied in several microorganisms, including *E. coli* (Andersen et al., 1998) and *B. subtilis* (Griffith and Grossman, 2008; Wiegert and Schumann, 2001), has already been used to decrease the stability of transcription factors and improve the performance of genetic circuits (Stricker et al., 2008). We have therefore tagged the four ECFs with 11 SsrA-tag variants reported to confer different protein stabilities (Andersen et al., 1998; Griffith and Grossman, 2008; Wiegert and Schumann, 2001) and subsequently tested the behavior of the resulting switches.

Again, the four switches responded differently to SsrA-tagging. The ECF105 switch was most sensitive, with all tagged variants being inactive (Figure 2; closed squares), whereas BL00106 was the most insensitive, with only three variants imposing major changes in switch behavior: LAA renders the switch inactive, whereas DVS and ASV cause an increase in baseline and maximal output (Figure 2). In the case of SVEN_0399, all variants caused a reduction in the switch's dynamic range with three of them (LAA, LVA, and AAV) resulting in the complete inactivation of the switch (Figure 2). The most complex scenario is observed for BL04030. Four variants (LAA, LVA, LDD, and ASV) have no effects on the dynamic range of the switches but cause the loss of the digital behavior exhibited by the untagged ECF (Figure S9). Three variants (LAD, DAG, and AAV) cause its inactivation (Figure 2), whereas the remaining four variants (ISV, ISS, HHA, and DVS) cause an increase in baseline and maximal output, and also the loss of the digital behavior exhibited by the untagged ECF (Figures 2 and S9).

Reducing the ECF-Target Promoter Size

Transcription initiation starts with binding of the RNApol to its target promoter. Several contact points are made between RNApol subunits and the promoter (Browning and Busby, 2016; Yuzenkova et al., 2011): the C-terminal domain of the α subunit contacts the promoter UP element (located approximately at positions −37 to −58); the conserved region 4 of the σ subunit contacts the −35 element (positions −35 to −30), whereas its region 2 contacts the −10 element (positions −12 to −7). In addition, the β′ subunit contacts the Z-element (positions −24 to −18 in the spacer region between −35 and −10 elements). Using the switches of Figure 1 as starting point, we have varied the length of the DNA fragment carrying the promoter. In all cases we have tested shorter fragments, except in the case of SVEN_0399, in which a bigger fragment (−129 to +71) was also tested because the initial switch was built with a smaller promoter fragment.

Two major conclusions can be drawn from the vast array of tested BL00106 target promoter fragments (Figure 2; open squares): first, changes in baseline can be achieved by varying the length of the upstream region (compare fragments starting at positions −122, −56, and −35). Second, changes in maximal output can be achieved by varying the length of the downstream regions (for each starting position compare fragments ending at positions +78, +30, +10, +17, and +1) (Figure S10).

For the other ECF switches, we obtained a number of surprising results: all shorter promoter fragments for BL04030 and ECF105 resulted in inactive switches (Figure 2), whereas the longest fragment for SVEN_0399 (−129 to +71) also failed to support the activity of the switch (Figure 2). The fact that a DNA fragment containing all necessary RNApol contact regions is not sufficient for switch activity is puzzling. One should note that the BL00106 target promoter is the only one for which the transcriptional start site has been

experimentally determined (Wecke et al., 2012). Hence, the contact regions for the BL04030 and ECF105 σ factors might have been incorrectly predicted or other recognition sequences for binding of additional transcription factors might be necessary. As for the inactivity of the $P_{SVEN\_0399\ -129\ to\ +71}$ promoter, we hypothesize that this is due to the high GC content of the *S. venezuelae* promoter, which hampers transcription initiation in the low GC *B. subtilis*.

For both BL00106 and SVEN_0399, our results further underscore the previously described crucial importance of the UP element for efficient transcription initiation (Rhodius et al., 2013): if this element is not included (Figure 2; "−35 to xx" fragments) the activity of the switch is drastically reduced.

Antisense Transcription

Antisense transcription occurs when promoters are located downstream and oriented in the opposite direction of genes. This particular design can influence gene expression through transcriptional interference (Bordoy et al., 2016; Brophy and Voigt, 2016). In this work we investigated the influence of antisense transcription in the behavior of the ECF switches by introducing an antisense promoter downstream of the ECF genes. We chose five promoters of different strengths: the *B. subtilis* σ^A-dependent promoters P_{veg} (very strong), P_{lepA} (strong), and P_{liaG} (weak) (Jordan et al., 2006; Michna et al., 2016); the intermediately strong *B. subtilis* σ^W-dependent promoter P_{sigW} (Helmann and Moran, 2002); and the *E. coli* σ^A-dependent promoter P_{J23101} (Anderson laboratory, http://parts.igem.org/Promoters/Catalog/Anderson), which is almost inactive in *B. subtilis* (Radeck et al., 2013).

Again, the ECF switches respond differently to this modification (Figure 2; crosses). The BL00106 switch is rather robust to transcriptional interference, whereas the ECF105 and SVEN_0399 switches are the most sensitive, resulting in a severe reduction of dynamic range, mostly due to an increased basal activity (Figure 2, crosses). Again, the BL04030 switch shows the most complex behavior: transcriptional interference decreased the dynamic range, either by reducing the maximal output (P_{sigW} and P_{veg}) or by increasing the basal activity (P_{lepA}, P_{liaG} and P_{J23101}). Moreover, in all cases but under P_{veg} interference, the digital behavior of the BL04030 switch is lost (Figure S11).

Overall Robustness of the Switches to Genetic Perturbations

The results from the previous sections demonstrate that the different modifications resulted in rather switch-specific alterations in their behavior that preclude easy generalizations. The plots shown in Figure 2 provide an overview of the effect of these alterations on the baseline, maximal output, and maximal fold-induction of the switches. Each point represents one type of alteration relative to the default switch, i.e., the initial design as shown in Figure 1B (represented as a black X in Figure 2). The distribution of these points in the three-dimensional space therefore provides a measure of switch robustness toward modifications (Figure S12).

Based on this, BL00106 and BL04030 are the two most robust switches, whereas ECF105 and SVEN_0399 are the most sensitive ones. For ECF105, most alterations cause its inactivation. A similar trend can be seen for SVEN_0399, for which a decrease in performance (increase in baseline, decrease in maximal output, and maximal fold-induction) is very pronounced. The reasons behind and implications of this behavior will be discussed in the next section.

DISCUSSION

From a conceptual perspective, the engineering of the σ subunit of RNApol indeed holds great potential as a universal way of controlling bacterial transcription initiation. In agreement with this, several groups have implemented σ-factor-based genetic switches and circuits (Chen and Arkin, 2012; Pinto et al., 2018; Rhodius et al., 2013; Shin and Noireaux, 2012). Despite these first successes, little is still known about the behavior of these regulatory units in less isolated frameworks.

Here, we report on our attempts to implement ECF-based switches from different origins in *B. subtilis*. In contrast to the results obtained for ECF switch implementation in *E. coli* (Rhodius et al., 2013), but in line with our preliminary observations (Pinto et al., 2018), only 4 of 46 constructed ECF switches were active. This high failure rate (over 82% inactive switches) does not seem to be due to: (1) the nature of the promoter used to induce expression, because inactive switches were built with both P_{xylA} and P_{lial}; (2) the

deleterious effects of codon optimization on expression of the ECFs, because those from *E. coli* were not subjected to codon optimization and the resulting switches were also inactive; or (3) the unfeasibility of implementing ECFs from specific ECF groups, given that the ECF41 (BL00106) switch from *B. licheniformis* is active but none of the ECF41 switches from *S. meliloti* and *S. venezuelae* are. The overall trend seems to be that only ECFs from the same phylum, Firmicutes (here *B. licheniformis* and *B. cereus*), could successfully be implemented in *B. subtilis*. The reasons behind this apparent narrower range of acceptance of heterologous σ factors are currently unknown, and additional work will be necessary. However, we can postulate that the amino acid differences observed in the RNApol catalytic subunits of different phyla (Lane and Darst, 2010a) might generate a stricter environment for RNApol-σ factor interaction in *B. subtilis*. Another possibility concerns the Firmicutes-specific δ subunit, which is involved in decreasing the affinity of the RNApol to DNA (López De Saro et al., 1999) and therefore might impair the ability of σ factors not evolved in its presence to form a productive transcriptional complex. For the specific case of ECFs originating from high-GC organisms, we can also conceive the requirement of additional factors whose function concerns the stabilization of high-GC open complexes, as is the case in other high-GC organisms (Bae et al., 2015; Hu et al., 2014).

For the four active switches, we have systematically investigated the effect of genetically introduced perturbations on their behavior, by changing: (1) the copy number of each or both constituent transcriptional units, (2) the inducible promoter driving ECF expression, (3) the stability of the ECF protein, (4) the length of the DNA fragment containing the promoter, and (5) antisense transcription over the ECF coding gene and against the inducible promoter. The extensive variability we observed in the response of each ECF switch to a given alteration, and even to alterations of the same type, highlights the complexity of the regulation of ECF switch activity, which we cannot fully predict still. Hence a comprehensive analysis of the different factors influencing ECF activity *in vivo* is still required for each new ECF switch.

However, despite the high variability in responses between the four ECF switches, we could, nevertheless, extract some common trends on how to design ECF switches. An increase in copy number of any (or both) of the transcriptional units increased the baseline, which is in agreement with the results of implementing ECF timer circuits (Pinto et al., 2018). Accordingly, ECF switches for synthetic biology applications should be integrated into the chromosome rather than applied as multi-copy plasmid-borne transcriptional units. This will ensure balanced and tightly controlled expression because the copy number of the switch directly correlates with that of the chromosome. In addition, the switch can then be stably maintained without the need for constant selective pressure.

The choice of the inducible promoter used to drive ECF expression is another important aspect to consider when designing an ECF switch, as we observed that the shape of the output curves of the ECF switches closely follows that of the promoters driving their expression (Figures 1 and S4). This suggests that the stability of the ECF is equivalent to or lower than that of the reporter, as otherwise we would expect that a stable response of the switch is maintained by the ECF even after transcription of its coding gene has stopped. We have previously determined the half-life of the luminescence reporter signal to be between 4 and 5 minutes (Radeck et al., 2013). This suggests that the stability of our ECFs is also only a few minutes, which indeed has been reported for other σ factors (Zhou and Gottesman, 2006).

Reduction of transcription factor stability is an important parameter that has already been exploited in *E. coli* (Stricker et al., 2008) and *E. coli* cell-free systems (Shin and Noireaux, 2012) to increase the temporal resolution of oscillators and reduce the baseline of genetic switches. Here, we have investigated the behavior of our ECF switches when the ECF was tagged for degradation by addition of SsrA tags. It is tempting to suggest that the observed complete inactivation of our tagged ECF switches (Figures S9) is the result of further reducing the already low stability of ECFs. Therefore a deliberate reduction of ECF stability does not improve the performance of ECF switches, in contrast to other transcription factors.

Antisense transcription is another mechanism by which transcriptional regulation can be influenced. It is naturally found in *B. subtilis* (Eiamphungporn and Helmann, 2009) and has already been exploited in the scope of synthetic biology (Bordoy et al., 2016; Brophy and Voigt, 2016). Here we have investigated

the effect of having two divergently oriented promoters flanking the ECF-coding gene and observed that the effects upon the performance of the ECF switches increase with the strength of the antisense promoter. Hence, the possibility of antisense transcription is another aspect to keep in mind and avoid (e.g., by insulating the ECF σ factor coding gene with strong antisense terminators) when implementing an ECF switch.

In conclusion, our study shows that *B. subtilis* has a very narrow phylogenetic acceptance range for heterologous ECFs and that the effects of genetic variations on switch performance needs to be evaluated for each ECF individually. However, despite the observed individual variations, we also observe overall trends that allow us to derive the following design rules for ECF switches for implementation in *B. subtilis*: (1) ECFs from closely related organisms should be chosen; (2) the ECF switch should be implemented in single copy; (3) the inducible promoter driving the ECF expression should be chosen according to the type of response desired (e.g., constant or transient); (4) the ECF stability should not be decreased, e.g., by degradation tags; (5) the UP element should be included in the ECF target promoter, although we should notice that the importance of a potential UP element will depend on the precise nature of the promoter and the strength of its interaction with the RNApol; and (6) antisense transcription should be avoided.

The study presented here reports a systematic characterization of ECF-based genetic switches under different genetic environments. And although *in vivo* synthetic genetic circuits are never completely uncoupled from the host cell's physiology, we want robust circuits that are minimally affected by that. Having information about the robustness of the switches we employ in our circuits allow us to better choose them, to better design the circuit, and to better predict its behavior.

Limitations of the Study

With this study we have shown that *B. subtilis* has a reduced phylogenetic range of acceptance of heterologous ECF switches, but no conclusions about the reasons behind this observation can be drawn from our data. However, given the relevance of this question to the understanding of bacterial transcription initiation, it will be a topic of further research in our group. Furthermore, we have comprehensively assessed the effect of alternative genetic switch designs, but very few of these alterations resulted in an increase in the performance of the switch, which suggests that efforts toward optimization of ECF switches will be better used in the incorporation of partner proteins (e.g., anti-sigma factors) than on design changes.

METHODS

All methods can be found in the accompanying Transparent Methods supplemental file.

SUPPLEMENTAL INFORMATION

Supplemental Information can be found online at https://doi.org/10.1016/j.isci.2019.03.001.

ACKNOWLEDGMENTS

We would like to acknowledge Andreas Sichert, Christopher Sauer, and Susanne Gebhard for generating and providing some of the plasmids used in this study. Work in the Mascher laboratory on ECFs is supported by grants from the Deutsche Forschungsgemeinschaft (DFG grant MA2837/2-2) and the Bundeministerium für Bildung und Forschung (BMBF) in the framework of the ERAnet Synthetic Biology (project ERASynBio2-ECFexpress). D.P. has received funding from the People Program (Marie Curie Actions) of the European Union's Seventh Framework Programme (FP7/2007-2013) under REA grant agreement no. 628509. Q.L. was funded by the China Scholarship Council (CSC). D.A. was funded by the Ciência sem Fronteiras program. F.D. was financially supported by the Graduate Academy of the TU Dresden. None of the funding bodies intervene in the design of the study and collection, analysis, and interpretation of data or in writing the manuscript.

AUTHOR CONTRIBUTIONS

D.P. and T.M. designed the study. D.P., F.D., F.F., Q.L., and D.A. collected the data. D.P. analyzed the data. D.P. and T.M. interpreted the data and drafted the manuscript. All authors read and approved the final manuscript.

DECLARATION OF INTERESTS

The authors declare that they have no competing interests.

Received: December 12, 2018
Revised: February 14, 2019
Accepted: March 1, 2019
Published: March 29, 2019

REFERENCES

Alper, H., Fischer, C., and Nevoigt, E. (2005). Tuning genetic control through promoter engineering. Proc. Natl. Acad. Sci. U S A *102*, 12678–12683.

Andersen, J.B., Sternberg, C., Poulsen, L.K., Petersen Bjørn, S., Givskov, M., and Molin, S. (1998). New unstable variants of green fluorescent protein for studies of transient gene expression in bacteria. Appl. Environ. Microbiol. *64*, 2240–2246.

Annunziata, F., Matyjaszkiewicz, A., Fiore, G., Grierson, C.S., Marucci, L., di Bernardo, M., and Savery, N.J. (2017). An orthogonal multi-input integration system to control gene expression in *Escherichia coli*. ACS Synth. Biol. *6*, 1816–1824.

Bae, B., Chen, J., Davis, E., Leon, K., Darst, S.A., and Campbell, E.A. (2015). CarD uses a minor groove wedge mechanism to stabilize the RNA polymerase open promoter complex. Elife *4*, 1–19.

Bervoets, I., Van Brempt, M., Van Nerom, K., Van Hove, B., Maertens, J., De Mey, M., and Charlier, D. (2018). A sigma factor toolbox for orthogonal gene expression in *Escherichia coli*. Nucleic Acids Res. *46*, 1–12.

Bibb, M.J., Domonkos, A., Chandra, G., and Buttner, M.J. (2012). Expression of the chaplin and rodlin hydrophobic sheath proteins in *Streptomyces venezuelae* is controlled by σ(BldN) and a cognate anti-sigma factor, RsbN. Mol. Microbiol. *84*, 1033–1049.

Bordoy, A.E., Varanasi, U.S., Courtney, C.M., and Chatterjee, A. (2016). Transcriptional interference in convergent promoters as a means for tunable gene expression. ACS Synth. Biol. *5*, 1331–1341.

Brophy, J.A., and Voigt, C.A. (2016). Antisense transcription as a tool to tune gene expression. Mol. Syst. Biol. *12*, 854.

Browning, D.F., and Busby, S.J.W. (2016). Local and global regulation of transcription initiation in bacteria. Nat. Rev. Microbiol. *14*, 638–650.

Chen, D., and Arkin, A.P. (2012). Sequestration-based bistability enables tuning of the switching boundaries and design of a latch. Mol. Syst. Biol. *8*, 620.

Dufour, Y.S., Imam, S., Koo, B.-M., Green, H.A., and Donohue, T.J. (2012). Convergence of the transcriptional responses to heat shock and singlet oxygen stresses. PLoS Genet. *8*, e1002929.

Eiamphungporn, W., and Helmann, J.J.D. (2009). Extracytoplasmic function sigma factors regulate expression of the *Bacillus subtilis yabE* gene via a cis-acting antisense RNA. J. Bacteriol. *191*, 1101–1105.

El-Gebali, S., Mistry, J., Bateman, A., Eddy, S.R., Luciani, A., Potter, S.C., Qureshi, M., Richardson, L.J., Salazar, G.A., Smart, A., et al. (2019). The Pfam protein families database in 2019. Nucleic Acids Res. *47*, D427–D432.

Feklístov, A., Sharon, B.D., Darst, S.A., and Gross, C.A. (2014). Bacterial sigma factors: a historical, structural, and genomic perspective. Annu. Rev. Microbiol. *68*, 357–376.

Gangaiah, D., Zhang, X., Baker, B., Fortney, K.R., Liu, Y., Munson, R.S., and Spinola, S.M. (2014). *Haemophilus ducreyi* RpoE and CpxRA appear to play distinct yet complementary roles in regulation of envelope-related functions. J. Bacteriol. *196*, 4012–4025.

Gärtner, D., Geissendörfer, M., and Hillen, W. (1988). Expression of the *Bacillus subtilis xyl* operon is repressed at the level of transcription and is induced by xylose. J. Bacteriol. *170*, 3102–3109.

Griffith, K.L., and Grossman, A.D. (2008). Inducible protein degradation in *Bacillus subtilis* using heterologous peptide tags and adaptor proteins to target substrates to the protease ClpXP. Mol. Microbiol. *70*, 1012–1025.

Helmann, J.D., and Moran, C.P. (2002). RNA polymerase and sigma factors. In *Bacillus subtilis* and its Closest Relatives, A. Sonenshein, R. Losick, and J. Hoch, eds. (ASM Press), pp. 289–312, https://doi.org/10.1128/9781555817992.ch21.

Hu, Y., Morichaud, Z., Perumal, A.S., Roquet-Baneres, F., and Brodolin, K. (2014). Mycobacterium RbpA cooperates with the stress-response σ^B subunit of RNA polymerase in promoter DNA unwinding. Nucleic Acids Res. *42*, 10399–10408.

Jordan, S., Junker, A., Helmann, J.D., and Mascher, T. (2006). Regulation of LiaRS-dependent gene expression in *Bacillus subtilis*: identification of inhibitor proteins, regulator binding sites, and target genes of a conserved cell envelope stress-sensing two-component system. J. Bacteriol. *188*, 5153–5166.

Karzai, a W., Roche, E.D., and Sauer, R.T. (2000). The SsrA-SmpB system for protein tagging, directed degradation and ribosome rescue. Nat. Struct. Biol. *7*, 449–455.

Kraus, A., Hueck, C., Gartner, D., and Hillen, W. (1994). Catabolite repression of the *Bacillus subtilis xyl* operon involves a *cis* element functional in the context of an unrelated sequence, and glucose exerts additional *xylR*-dependent repression. J. Bacteriol. *176*, 1738–1745.

Lane, W.J., and Darst, S.A. (2010a). Molecular evolution of multisubunit RNA polymerases: sequence analysis. J. Mol. Biol. *395*, 671–685.

Lane, W.J., and Darst, S.A. (2010b). Molecular evolution of multisubunit RNA polymerases: structural analysis. J. Mol. Biol. *395*, 686–704.

Lepesant, J.A., Billault, A., Kejzlarová-Lepesant, J., Pascal, M., Kunst, F., and Dedonder, R. (1974). Identification of the structural gene for sucrase in *Bacillus subtilis* Marburg. Biochimie *56*, 1465–1470.

López De Saro, F.J., Yoshikawa, N., and Helmann, J.D. (1999). Expression, abundance, and RNA polymerase binding properties of the δ factor of *Bacillus subtilis*. J. Biol. Chem. *274*, 15953–15958.

Mao, X.-M., Sun, N., Wang, F., Luo, S., Zhou, Z., Feng, W.-H., Huang, F.-L., and Li, Y.-Q. (2013). Dual positive feedback regulation of protein degradation of an extra-cytoplasmic function σ factor for cell differentiation in *Streptomyces coelicolor*. J. Biol. Chem. *288*, 31217–31228.

Mascher, T. (2013). Signaling diversity and evolution of extracytoplasmic function (ECF) σ factors. Curr. Opin. Microbiol. *16*, 148–155.

Mascher, T., Zimmer, S.L., Smith, T., and Helmann, J.D. (2004). Antibiotic-inducible promoter regulated by the cell envelope stress-sensing two-component system LiaRS of *Bacillus subtilis*. Antimicrob. Agents Chemother. *48*, 2888–2896.

Mathew, R., and Chatterji, D. (2006). The evolving story of the omega subunit of bacterial RNA polymerase. Trends Microbiol. *14*, 450–455.

Meyer, A.J., Ellefson, J.W., and Ellington, A.D. (2015). Directed evolution of a panel of orthogonal T7 RNA polymerase variants for *in vivo* or *in vitro* synthetic circuitry. ACS Synth. Biol. *4*, 1070–1076.

Michna, R.H., Zhu, B., Mäder, U., and Stülke, J. (2016). SubtiWiki 2.0–an integrated database for the model organism *Bacillus subtilis*. Nucleic Acids Res. *44*, D654–D662.

Nielsen, A.A.K., Der, B.S., Shin, J., Vaidyanathan, P., Paralanov, V., Strychalski, E.A., Ross, D., Densmore, D., and Voigt, C.A. (2016). Genetic circuit design automation. Science *352*, aac7341.

Pinto, D., and Mascher, T. (2016). The ECF classification: a phylogenetic reflection of the regulatory diversity in the extracytoplasmic function sigma factor protein family. In Stress and Environmental Regulation of Gene Expression and Adaptation in Bacteria, First Edition, Frans J. de Bruijn, ed. (John Wiley & Sons, Inc), pp. 64–96.

Pinto, D., Vecchione, S., Wu, H., Mauri, M., Mascher, T., and Fritz, G. (2018). Engineering orthogonal synthetic timer circuits based on extracytoplasmic function σ factors. Nucleic Acids Res. *46*, 7450–7464.

Radeck, J., Kraft, K., Bartels, J., Cikovic, T., Dürr, F., Emenegger, J., Kelterborn, S., Sauer, C., Fritz, G., Gebhard, S., and Mascher, T. (2013). The Bacillus BioBrick Box: generation and evaluation of essential genetic building blocks for standardized work with *Bacillus subtilis*. J. Biol. Eng. *7*, 29.

Rhodius, V.A., Segall-shapiro, T.H., Sharon, B.D., Ghodasara, A., Orlova, E., Tabakh, H., Burkhardt, D.H., Clancy, K., Peterson, T.C., Gross, C.A., and Voigt, C.A. (2013). Design of orthogonal genetic switches based on a crosstalk map of σs, anti-σs, and promoters. Mol. Syst. Biol. *9*, 702.

Sauer, C., Syvertsson, S., Bohorquez, L.C., Cruz, R., Harwood, C.R., van Rij, T., and Hamoen, L.W. (2016). Effect of genome position on heterologous gene expression in *Bacillus subtilis*: an unbiased analysis. ACS Synth. Biol. *5*, 942–947.

Schmalisch, M., Maiques, E., Nikolov, L., Camp, A.H., Chevreux, B., Muffler, A., Rodriguez, S., Perkins, J., and Losick, R. (2010). Small genes under sporulation control in the *Bacillus subtilis* genome. J. Bacteriol. *192*, 5402–5412.

Shin, J., and Noireaux, V. (2012). An *E. coli* cell-free expression toolbox: application to synthetic gene circuits and artificial cells. ACS Synth. Biol. *1*, 29–41.

Shipkowski, S., and Brenchley, J.E. (2006). Bioinformatic, genetic, and biochemical evidence that some glycoside hydrolase family 42 beta-galactosidases are arabinogalactan type I oligomer hydrolases. Appl. Environ. Microbiol. *72*, 7730–7738.

Stanton, B.C., Nielsen, A.A.K., Tamsir, A., Clancy, K., Peterson, T., and Voigt, C.A. (2014). Genomic mining of prokaryotic repressors for orthogonal logic gates. Nat. Chem. Biol. *10*, 99–105.

Staroń, A., Sofia, H.J., Dietrich, S., Ulrich, L.E., Liesegang, H., and Mascher, T. (2009). The third pillar of bacterial signal transduction: classification of the extracytoplasmic function (ECF) sigma factor protein family. Mol. Microbiol. *74*, 557–581.

Stricker, J., Cookson, S., Bennett, M.R., Mather, W.H., Tsimring, L.S., and Hasty, J. (2008). A fast, robust and tunable synthetic gene oscillator. Nature *456*, 516–519.

Toymentseva, A.A., Schrecke, K., Sharipova, M.R., and Mascher, T. (2012). The LIKE system, a novel protein expression toolbox for *Bacillus subtilis* based on the *lial* promoter. Microb. Cell Fact. *11*, 143.

Toyoda, K., Teramoto, H., Yukawa, H., and Inui, M. (2015). Expanding the regulatory network governed by the extracytoplasmic function sigma factor σ^H in *Corynebacterium glutamicum*. J. Bacteriol. *197*, 483–496.

Wecke, T., Halang, P., Staroń, A., Dufour, Y.S., Donohue, T.J., Mascher, T., Wecke, T., Halang, P., Staro, A., and Mascher, T. (2012). Extracytoplasmic function σ factors of the widely distributed group ECF41 contain a fused regulatory domain. Microbiologyopen *1*, 194–213.

Wiegert, T., and Schumann, W. (2001). SsrA-mediated tagging in *Bacillus subtilis*. J. Bacteriol. *183*, 3885–3889.

Yuzenkova, Y., Tadigotla, V.R., Severinov, K., and Zenkin, N. (2011). A new basal promoter element recognized by RNA polymerase core enzyme. EMBO J. *30*, 3766–3775.

Zhou, Y., and Gottesman, S. (2006). Modes of regulation of RpoS by H-NS. J. Bacteriol. *188*, 7022–7025.

ISCI, Volume *13*

Supplemental Information

Extracytoplasmic Function σ Factors Can Be Implemented as Robust Heterologous Genetic Switches in *Bacillus subtilis*

Daniela Pinto, Franziska Dürr, Friederike Froriep, Dayane Araújo, Qiang Liu, and Thorsten Mascher

I. Transparent methods

I.1 Selection of ECFs

Complete proteomes of *S. venezuelae* ATCC 10712, *S. meliloti* 1021, *E. coli* K-12 DH10β, *B. licheniformis* ATCC 14580, *B. cereus* ATCC 10987, and *B. subtilis* 168 were obtained from the Protein database of the National Center for Biotechnology Information (https://www.ncbi.nlm.nih.gov/protein). Protein sequences were submitted to the ECFfinder (http://ecf.g2l.bio.uni-goettingen.de:8080/ECFfinder/) (Staroń et al., 2009) for identification and classification of ECFs. Unclassified ECFs were then further analyzed for similarity with those of the remaining 28 groups (Gómez-Santos et al., 2011; Huang et al., 2015; Jogler et al., 2012; Pinto and Mascher, 2016) not included in the ECFfinder tool and classified as belonging of one of those groups when high sequence and genomic context similarities were observed. A subset of ECFs, from groups not present in *B. subtilis* 168 and from which putative ECF target promoters could be predicted accordingly to previously determined group specific putative target promoter motifs (Gómez-Santos et al., 2011; Huang et al., 2015; Jogler et al., 2012; Pinto and Mascher, 2016; Staroń et al., 2009), were selected for implementation into *B. subtilis* 168 (Figure 1).

Target promoter sequences were selected for each ECF. The target promoter for BL00106 was that previously determined (Wecke et al., 2012). For the remaining ECFs we took under consideration the auto-regulatory nature of ECFs and selected the intergenic sequence immediately upstream of the operons encoding the selected ECFs. The presence of a sequence similar to the target promoter motifs suggested for the ECF groups to which the selected ECFs belong to (Pinto and Mascher, 2016) was manually confirmed.

I.2 Strain generation

E. coli strains DH5α (F$^-$ *endA1 glnV44 thi-1 recA1 relA1 gyrA96 deoR nupG purB20* φ80d*lacZ*ΔM15 Δ(*lacZYA-argF*)U169, hsdR17($r_K^- m_K^+$), λ$^-$), DH10β (F$^-$ *endA1 deoR*$^+$ *recA1 galE15 galK16 nupG rpsL* Δ*(lac)X74* φ80*lacZΔM15 araD139* Δ*(ara,leu)7697 mcrA* Δ*(mrr-hsdRMS-mcrBC)* Str^R λ$^-$) and XL1-Blue (endA1 gyrA96(nal^R) thi-1 recA1 relA1 lac glnV44 F'[::Tn10 proAB$^+$ lacI^q Δ(lacZ)M15] hsdR17(r_K^- m_K^+)) were used for cloning. Cells were grown in LB medium, and ampicillin (100 μg/ml) was added for selection and maintenance of plasmids.

Plasmids were generated according to BioBrick standards. ECF encoding genes and target promoters from *B. licheniformis* DSM13, *B. cereus* environmental isolate and *E. coli* DH10β were amplified from preparations of total DNA with the primers listed on table S3. ECF encoding genes from *S. venezuelae* ATCC 10712 and *S. meliloti* 1021 were codon optimized for *B. subtilis* according to the codon usage frequency characteristic of each organism (table S6). Forbidden restriction sites accordingly to RFC10 BioBrick standard were removed, the RBS sequence and the N-terminal FLAG tag was added upstream. Genes were synthetized by GeneArt and later cloned into the appropriate vectors. ECF target promoters were obtain by annealing of complementary oligonucleotides (table S4) generating the appropriate overhangs for cloning into the RFC10 BioBrick standard compatible vectors. A complete list of the generated plasmids can be found in table S2.

B. subtilis 168 strain was used for all experiments. The relevant generated plasmids were introduced in *B. subtilis* 168 by transformation and the resulting strains were grown at 37°C in LB medium supplemented with the relevant antibiotics for selection: erythromycin and lincomycin (1 and 25 μg/ml, respectively) for selection of the mls^R strains and chloramphenicol (5 μg/ml) for selection of the cm^R strains.

I.3 Measurement of growth and switch behavior

Overnight cultures of *B. subtilis* 168 strains harboring ECF-based switched containing σ factors of *B. licheniformis* DSM13 and *B. cereus* environmental isolate were diluted 1:165 in fresh LB medium and incubated at 30°C with shaking for 4 hours. The exponentially growing cultures were then diluted to an optical density at 600nm (OD_{600}) of 0.05 and incubated at 30°C. Both growth and promoter output were monitored every 5 minutes for 16 hours by measuring OD_{600} and luminescence in a BioTek Synergy 2 microtiter plate reader. After 1 hour, induction of ECF expression was accomplished through medium supplementation with 0.5% xylose (for strains in which expression of the ECF coding gene was dependent on P_{xylA}) or 10 μg/mL of

bacitracin (for strains in wish expression of the ECF coding gene was dependent on P_{lial}). Growth and switch behavior of all strains was additionally performed on MCSE medium (Radeck et al., 2013) at 37°C.

I.4 Data analysis

To generate growth curves the OD_{600} values were used. In each assay, the average OD_{600} value of three negative controls (sterile medium) was subtracted to all time-points of all cultures. The operations described here can be represented by $OD600_{Sa\ tx} = \frac{\sum_{R=1}^{3}\left(OD600raw_{Sa\ tx} - \frac{\sum_{R=1}^{3}\sum_{t=0}^{960} OD600raw_{blank}}{3x960}\right)}{3}$ in which 'S' represents the strain, 't' the time point and 'R' represents the replicate. The average of three independent experiments was then plotted against time expressed in minutes. To generate luminescence curves the luminescence values expressed as relative luminescence units were used. In each experiment, the luminescence values were normalized by the OD_{600}. This operation can be represented by $RLU/_{OD600} = \frac{\sum_{R=1}^{3}\frac{RLU_{Sa\ tx}}{OD600_{Sa\ tx}}}{3}$ following the same notation as before. The average of three independent experiments was then plotted against time expressed in minutes. To generate dose-response curves we first looked at the behavior of the inducible promoters P_{xylA}, *xylR*-P_{xylA} and P_{lial} and observed that in all cases the maximal output was achieved, in the conditions of the assay, 90 minutes after the addition of the inducer. For that reason, dose-response curves of all ECF-based switches were generated by plotting the average value of luminescence normalized by optical density against inducer concentration. In all cases, averages, standard deviations and coefficients of variation were calculated from three independent experiments. The switches were considered active when the promoter activity was consistently at least two-fold above background for at least three consecutive measurements.

II. Strains

All strains are listed in Table S1.

III. Plasmids

III.1 Plasmid list

All plasmids are listed in Table S2.

III.2 Plasmid maps

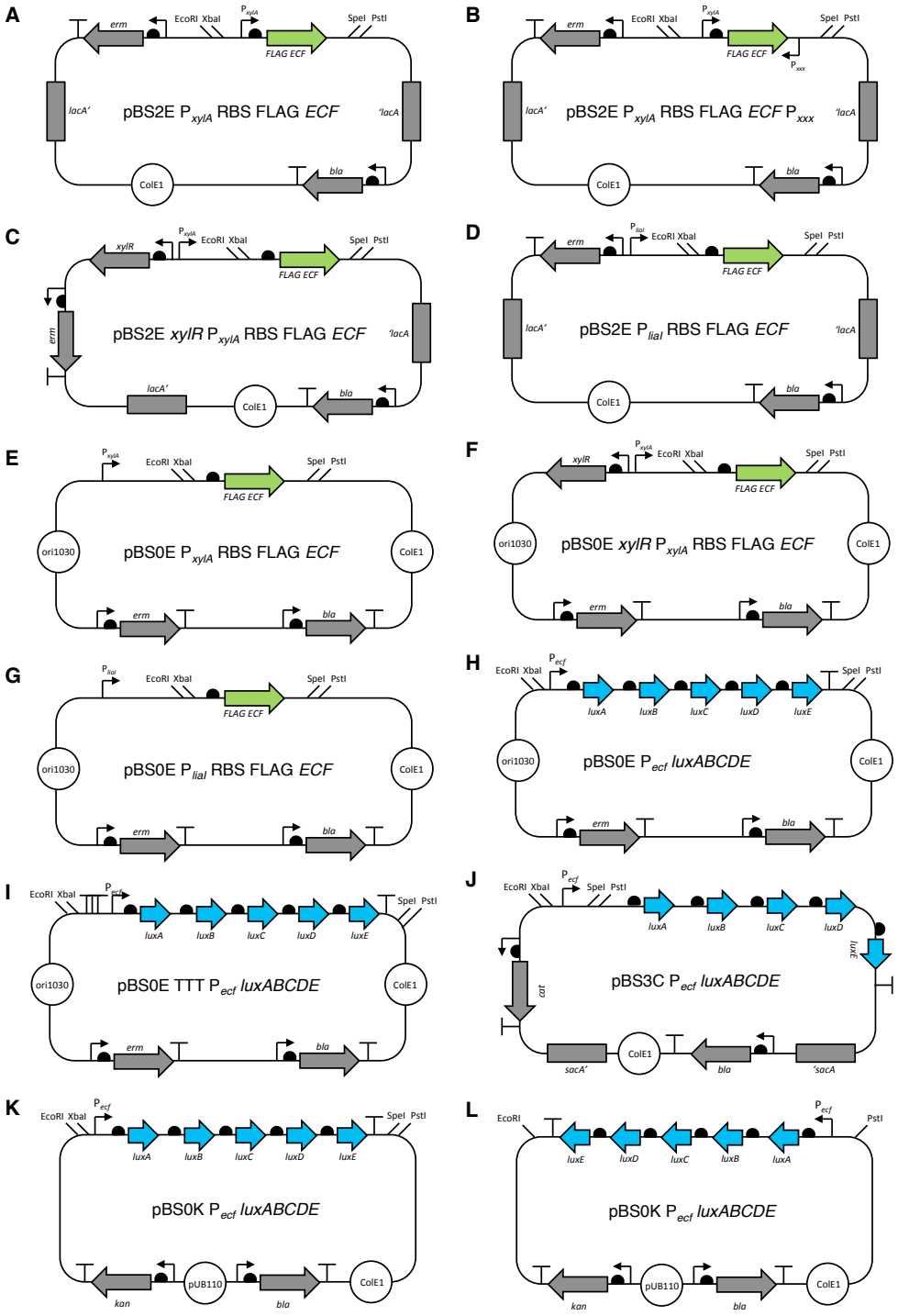

Figure S1. Maps of the plasmids used in this study, Related to Figure 1 and Figure 2. Rectangles represent homology regions that are necessary for homologous recombination into *B. subtilis* 168 chromosome. Circles represent origins of replication. Thick arrows represent open reading frames. 'T' represent terminators. Half circles represent ribosome binding sites. Thin arrows represent promoters. Oblique lines represent restriction sites.

III.3 Plasmid sequences

Plasmid sequences containing relevant annotations have been compiled in GenBank format in Data S1. Sequences are identified by plasmid name as in Table S2.

IV. Primers

Table S3. PCR primers used in this study, Related to Figure 2 and Figure 1.

Name	Description	Sequence*
TM3575	*BL00106* fwr	AGTCGAATTCGCGGCCGCTTCTAGAGAAGGAGGTGAGGATCT*ATGGATTATAAGGATCATGATGGTGATTATAAGGATCATGATATCGACTACAAAGACGATGACGACAAG*GAATATTATCGACAATATCATTC
TM3639	*BL00106* PstI- rev	CTTCTTGCGGGCAGACTGGAGTTCATTTATGCAGCGGTTTG
TM3640	*BL00106* PstI- fwr	CAAACCGCTGCATAAATGAACTCCAGTCTGCCCGCAAGAAG
TM3641	*BL00106* BsaI- rev	GCTCTTTCCATAGATCGGTCGCAAAGCGCTGCGCAC
TM3642	*BL00106* BsaI- fwr	GTGCGCAGCGCTTTGCGACCGATCTATGGAAAGAGC
TM3576	*BL00106* wt rev	ACGTACTAGTATTATATTTTAATGTGCTTCAGTTTATC
TM4181	*BL04030* fwr	AGTCTCTAGAAAGGAGGTGAGGATCT*ATGGATTATAAGGATCATGATGGTGATTATAAGGATCATGATATCGACTACAAAGACGATGACGACAAG*AATGAATTAGAACAGCAAGCGC
TM4182	*BL04030* rev	GTTTCTTCCTGCAGCGGCCGCTACTAGTACTAGGCAGCGCACCTC
TM4616	*ecf105* fwr	AGTCTCTAGAAAGGAGGTGAGGATCT*ATGGATTATAAGGATCATGATGGTGATTATAAGGATCATGATATCGACTACAAAGACGATGACGACAAG*CAAACATATCGTCACTATATTTTC
TM4613	*ecf105* rev	GTTTCTTCCTGCAGCGGCCGCTACTAGTATCATAGAAACTCTTCCTCCTTC
TM3532	*BL00106* (1-204aa) rev	AGTCACTAGTTCACACTTTTCCGCCGCCATCT
TM3577	*BL00106* (1-167aa) rev	ACGTACTAGTATTATTCTTCAACCGGCTGTG
TM4885	*BL00106*_LDD rev	GTTTCTTCCTGCAGCGGCCGCTACTAGTATTATTA**GTCGTCTAA**TGCTACGTTTTGGTTAAAACTGTTAGTTTTGCCTGCTATTTTAATGTGCTTCAG
TM4886	*BL00106*_LAD rev	GTTTCTTCCTGCAGCGGCCGCTACTAGTATTATTA**GTCGGCTAA**TGCTACGTTTTGGTTAAAACTGTTAGTTTTGCCTGCTATTTTAATGTGCTTCAG
TM4884	*BL00106*_ASV rev	GTTTCTTCCTGCAGCGGCCGCTACTAGTATTATTA**GACCGACGC**TGCTACGTTTTGGTTAAAACTGTTAGTTTTGCCTGCTATTTTAATGTGCTTCAG
TM4882	*BL00106*_AAV rev	GTTTCTTCCTGCAGCGGCCGCTACTAGTATTATTA**GACGGCCGC**TGCTACGTTTTGGTTAAAACTGTTAGTTTTGCCTGCTATTTTAATGTGCTTCAG
TM4988	*BL00106*_DAG rev	GTTTCTTCCTGCAGCGGCCGCTACTAGTATTATTA**CCCGGCGTC**TGCTACGTTTTGGTTAAAACTGTTAGTTTTGCCTGCTATTTTAATGTGCTTCAG
TM4989	*BL00106*_DVS rev	GTTTCTTCCTGCAGCGGCCGCTACTAGTATTATTA**CGAGACGTC**TGCTACGTTTTGGTTAAAACTGTTAGTTTTGCCTGCTATTTTAATGTGCTTCAG
TM4990	*BL00106*_ISS rev	GTTTCTTCCTGCAGCGGCCGCTACTAGTATTATTA**CGACGAAAT**TGCTACGTTTTGGTTAAAACTGTTAGTTTTGCCTGCTATTTTAATGTGCTTCAG
TM4991	*BL00106*_HHA rev	GTTTCTTCCTGCAGCGGCCGCTACTAGTATTATTA**GGCATGATG**TGCTACGTTTTGGTTAAAACTGTTAGTTTTGCCTGCTATTTTAATGTGCTTCAG
TM4992	*BL00106*_ISV rev	GTTTCTTCCTGCAGCGGCCGCTACTAGTATTATTA**GACCGAAAT**TGCTACGTTTTGGTTAAAACTGTTAGTTTTGCCTGCTATTTTAATGTGCTTCAG
TM4883	*BL00106*_LVA rev	GTTTCTTCCTGCAGCGGCCGCTACTAGTATTATTA**GGCGACTAA**TGCTACGTTTTGGTTAAAACTGTTAGTTTTGCCTGCTATTTTAATGTGCTTCAG
TM4775	*BL00106*_LAA rev	GTTTCTTCCTGCAGCGGCCGCTACTAGTATTATTA**GGCAGCTAA**TGCTACGTTTTGGTTAAAACTGTTAGTTTTGCCTGCTATTTTAATGTGCTTCAG
TM5745	*BL04030_LAA rev*	GTTTCTTCCTGCAGCGGCCGCTACTAGTATTATTA**GGCAGCTAA**TGCTACGTTTTGGTTAAAACTGTTAGTTTTGCCTGCGGCAGCGCACCTC
TM5746	*BL04030_AAV rev*	GTTTCTTCCTGCAGCGGCCGCTACTAGTATTATTA**GACGGCCGC**TGCTACGTTTTGGTTAAAACTGTTAGTTTTGCCTGCGGCAGCGCACCTC
TM5747	*BL04030_LVA rev*	GTTTCTTCCTGCAGCGGCCGCTACTAGTATTATTA**GGCGACTAA**TGCTACGTTTTGGTTAAAACTGTTAGTTTTGCCTGCGGCAGCGCACCTC
TM5748	*BL04030_ASV rev*	GTTTCTTCCTGCAGCGGCCGCTACTAGTATTATTA**GGCGACTAA**TGCTACGTTTTGGTTAAAACTGTTAGTTTTGCCTGCGGCAGCGCACCTC
TM5749	*BL04030_LDD rev*	GTTTCTTCCTGCAGCGGCCGCTACTAGTATTATTA**GTCGTCTAA**TGCTACGTTTTGGTTAAAACTGTTAGTTTTGCCTGCGGCAGCGCACCTC
TM5750	*BL04030_LAD rev*	GTTTCTTCCTGCAGCGGCCGCTACTAGTATTATTA**GTCGGCTAA**TGCTACGTTTTGGTTAAAACTGTTAGTTTTGCCTGCGGCAGCGCACCTC
TM5751	*BL04030_HHA rev*	GTTTCTTCCTGCAGCGGCCGCTACTAGTATTATTA**GGCATGATG**TGCTACGTTTTGGTTAAAACTGTTAGTTTTGCCTGCGGCAGCGCACCTC
TM5752	*BL04030_ISV rev*	GTTTCTTCCTGCAGCGGCCGCTACTAGTATTATTA**GACCGAAAT**TGCTACGTTTTGGTTAAAACTGTTAGTTTTGCCTGCGGCAGCGCACCTC
TM5753	*BL04030_ISS rev*	GTTTCTTCCTGCAGCGGCCGCTACTAGTATTATTA**GACCGAAAT**TGCTACGTTTTGGTTAAAACTGTTAGTTTTGCCTGCGGCAGCGCACCTC
TM5754	*BL04030_DAG rev*	GTTTCTTCCTGCAGCGGCCGCTACTAGTATTATTA**CCCGGCGTC**TGCTACGTTTTGGTTAAAACTGTTAGTTTTGCCTGCGGCAGCGCACCTC
TM5755	*BL04030_DVS rev*	GTTTCTTCCTGCAGCGGCCGCTACTAGTATTATTA**CGAGACGTC**TGCTACGTTTTGGTTAAAACTGTTAGTTTTGCCTGCGGCAGCGCACCTC
TM5756	*ECF105_LAA rev*	GTTTCTTCCTGCAGCGGCCGCTACTAGTATTATTA**GGCAGCTAA**TGCTACGTTTTGGTTAAAACTGTTAGTTTTGCCTGCTAGAAACTCTTCCTCCTTC
TM5757	*ECF105_AAV rev*	GTTTCTTCCTGCAGCGGCCGCTACTAGTATTATTA**GACGGCCGC**TGCTACGTTTTGGTTAAAACTGTTAGTTTTGCCTGCTAGAAACTCTTCCTCCTTC
TM5758	*ECF105_LVA rev*	GTTTCTTCCTGCAGCGGCCGCTACTAGTATTATTA**GGCGACTAA**TGCTACGTTTTGGTTAAAACTGTTAGTTTTGCCTGCTAGAAACTCTTCCTCCTTC
TM5759	*ECF105_ASV rev*	GTTTCTTCCTGCAGCGGCCGCTACTAGTATTATTA**GACCGACGC**TGCTACGTTTTGGTTAAAACTGTTAGTTTTGCCTGCTAGAAACTCTTCCTCCTTC
TM5760	*ECF105_LDD rev*	GTTTCTTCCTGCAGCGGCCGCTACTAGTATTATTA**GTCGTCTAA**TGCTACGTTTTGGTTAAAACTGTTAGTTTTGCCTGCTAGAAACTCTTCCTCCTTC
TM5761	*ECF105_LAD rev*	GTTTCTTCCTGCAGCGGCCGCTACTAGTATTATTA**GTCGGCTAA**TGCTACGTTTTGGTTAAAACTGTTAGTTTTGCCTGCTAGAAACTCTTCCTCCTTC
TM5762	*ECF105_HHA rev*	GTTTCTTCCTGCAGCGGCCGCTACTAGTATTATTA**GGCATGATG**TGCTACGTTTTGGTTAAAACTGTTAGTTTTGCCTGCTAGAAACTCTTCCTCCTTC
TM5763	*ECF105_ISV rev*	GTTTCTTCCTGCAGCGGCCGCTACTAGTATTATTA**GACCGAAAT**TGCTACGTTTTGGTTAAAACTGTTAGTTTT

		GCCTGCTAGAAACTCTTCCTCCTTC
TM5764	*ECF105_ISS rev*	GTTTCTTCCTGCAGCGGCCGCTACTAGTATTATTA**CGACGAAAT**TGCTACGTTTTGGTTAAAACTGTTAGTTTT GCCTGCTAGAAACTCTTCCTCCTTC
TM5765	*ECF105_DAG rev*	GTTTCTTCCTGCAGCGGCCGCTACTAGTATTATTA**CCCGGCGTC**TGCTACGTTTTGGTTAAAACTGTTAGTTTT GCCTGCTAGAAACTCTTCCTCCTTC
TM5766	*ECF105_DVS rev*	GTTTCTTCCTGCAGCGGCCGCTACTAGTATTATTA**CGAGACGTC**TGCTACGTTTTGGTTAAAACTGTTAGTTTT GCCTGCTAGAAACTCTTCCTCCTTC
TM5767	*SVEN_0399_fwr*	GTTTCTTCGAATTCGCGGCCGCTTCTAGAGAAGGAGGTGAGGATCTATG
TM5768	*SVEN_0399_LAA rev*	GTTTCTTCCTGCAGCGGCCGCTACTAGTATTATTA**GGCAGCTAA**TGCTACGTTTTGGTTAAAACTGTTAGTTTT GCCTGCGGTTGTTACCCCCATAC
TM5769	*SVEN_0399_AAV rev*	GTTTCTTCCTGCAGCGGCCGCTACTAGTATTATTA**GACGGCCGC**TGCTACGTTTTGGTTAAAACTGTTAGTTTT GCCTGCGGTTGTTACCCCCATAC
TM5770	*SVEN_0399_LVA rev*	GTTTCTTCCTGCAGCGGCCGCTACTAGTATTATTA**GGCGACTAA**TGCTACGTTTTGGTTAAAACTGTTAGTTTT GCCTGCGGTTGTTACCCCCATAC
TM5771	*SVEN_0399_ASV rev*	GTTTCTTCCTGCAGCGGCCGCTACTAGTATTATTA**GACCGACGC**TGCTACGTTTTGGTTAAAACTGTTAGTTTT GCCTGCGGTTGTTACCCCCATAC
TM5772	*SVEN_0399_LDD rev*	GTTTCTTCCTGCAGCGGCCGCTACTAGTATTATTA**GTCGTCTAA**TGCTACGTTTTGGTTAAAACTGTTAGTTTT GCCTGCGGTTGTTACCCCCATAC
TM5773	*SVEN_0399_LAD rev*	GTTTCTTCCTGCAGCGGCCGCTACTAGTATTATTA**GTCGGCTAA**TGCTACGTTTTGGTTAAAACTGTTAGTTTT GCCTGCGGTTGTTACCCCCATAC
TM5774	*SVEN_0399_HHA rev*	GTTTCTTCCTGCAGCGGCCGCTACTAGTATTATTA**GGCATGATG**TGCTACGTTTTGGTTAAAACTGTTAGTTTT GCCTGCGGTTGTTACCCCCATAC
TM5775	*SVEN_0399_ISV rev*	GTTTCTTCCTGCAGCGGCCGCTACTAGTATTATTA**GACCGAAAT**TGCTACGTTTTGGTTAAAACTGTTAGTTTT GCCTGCGGTTGTTACCCCCATAC
TM5776	*SVEN_0399_ISS rev*	GTTTCTTCCTGCAGCGGCCGCTACTAGTATTATTA**CGACGAAAT**TGCTACGTTTTGGTTAAAACTGTTAGTTTT GCCTGCGGTTGTTACCCCCATAC
TM5777	*SVEN_0399_DAG rev*	GTTTCTTCCTGCAGCGGCCGCTACTAGTATTATTA**CCCGGCGTC**TGCTACGTTTTGGTTAAAACTGTTAGTTTT GCCTGCGGTTGTTACCCCCATAC
TM5778	*SVEN_0399_DVS rev*	GTTTCTTCCTGCAGCGGCCGCTACTAGTATTATTA**CGAGACGTC**TGCTACGTTTTGGTTAAAACTGTTAGTTTT GCCTGCGGTTGTTACCCCCATAC
TM5179	*ECDH10B*_2741 fwr	GTTTCTTCTCTAGAGAAGGAGGTGAGGATCT*ATGGATTATAAGGATCATGATGGTGATTATAAGGATCATGATA TCGACTACAAAGACGATGACGACAAG*AGCGAGCAGTTAACGGAC
TM5180	*ECDH10B*_2741 rev	GTTTCTTCCTGCAGCGGCCGCTACTAGTATCAACGCCTGATAAGCGGTTG
TM5181	*ECDH10B*_4491 fwr	GTTTCTTCTCTAGAGAAGGAGGTGAGGATCT*ATGGATTATAAGGATCATGATGGTGATTATAAGGATCATGATA TCGACTACAAAGACGATGACGACAAG*TCTGACCGCGCCACTACC
TM5182	*ECDH10B*_4491 rev	GTTTCTTCCTGCAGCGGCCGCTACTAGTATAACCCATACTCCAGACGGAACAG
TM3526	$P_{ydfG\ -122}$ fwr	GTTTCTTCGAATTCGCGGCCGCTTCTAGAGCTTGGAATCCGGAAGGCGAT
TM3530	$P_{ydfG\ -56}$ fwr	GTTTCTTCGAATTCGCGGCCGCTTCTAGAGACATTAAAATATAACGTTTT
TM3643	$P_{ydfG\ -35}$ fwr	AGTCTCTAGATGTCACAAACTCCGTTTCTC
TM3529	$P_{ydfG\ +1}$ rev	GTTTCTTCCTGCAGCGGCCGCTACTAGTAACTTATATAACAAGAGAG
TM3528	$P_{ydfG\ +10}$ rev	GTTTCTTCCTGCAGCGGCCGCTACTAGTATAAGTGTTTCACTTATATAA
TM3785	$P_{ydfG\ +17}$ rev	GTTTCTTCCTGCAGCGGCCGCTACTAGTACCTCCTTTAAGTGTTTCAC
TM3786	$P_{ydfG\ +30}$ rev	GTTTCTTCCTGCAGCGGCCGCTACTAGTATTCCATGTCTATTCCTCC
TM3527	$P_{ydfG\ +78}$ rev	GTTTCTTCCTGCAGCGGCCGCTACTAGTACATTCCTCTGTATCCCTCAG
TM4183	$P_{BL04030}$ fwr	GTTTCTTCGAATTCGCGGCCGCTTCTAGAGTTTTTTGTTACAATCATAAAAAAAC
TM4184	$P_{BL04030}$ rev	GTTTCTTCCTGCAGCGGCCGCTACTAGTAAAAGAGGCCTCTTAC
TM4614	$P_{ecf105\ -158}$ fwr	GTTTCTTCGAATTCGCGGCCGCTTCTAGAGCACATCCTTTCTCCCTGTAAC
TM4615	$P_{ecf105\ +121}$ rev	GTTTCTTCCTGCAGCGGCCGCTACTAGTAAAGGATACGAAAAGCATGTTC
TM5785	$P_{SVEN\_0399\ -129}$ fwr	GTTTCTTCGAATTCGCGGCCGCTTCTAGAGGCAGCGGGGCCGGCGGGAC
TM5786	$P_{SVEN\_0399\ +71}$ rev	GTTTCTTCCTGCAGCGGCCGCTACTAGTATTGTGTCGTCGCTCGTGCGGGGCCGG

*RBS sequence is underlined; FLAG tag sequence is italicized; SsrA tag variants are highlighted in bold.

Table S4. Oligonucleotides for promoter generation, Related to Figure 1 and Figure 2.

Name	Description	Sequence*
TMP0068	P_{SVEN_0399} fwr	AATTCGCGGCCGCTTCTAGAGGGGGGCGCCGGTGACGAAGAGCGCTCCCATCCGCAGGGCCGTCCGCTACGAAGAA CGGGCGTA
	P_{SVEN_0399} rev	CTAGTACGCCCGTTCTTCGTAGCGGACGGCCCTGCGGATGGGAGCGCTCTTCGTCACCGGCGCCCCCCTCTAGAAG CGGCCGCG
TMP0053	P_{SVEN_4513} fwr	AATTCGCGGCCGCTTCTAGAGGCGCGCAGCTCGGCGGGGTCCTGCGGAACCGTGATCGCGTGGAGGTCGACGACCA TGTA
	P_{SVEN_4513} rev	CTAGTACATGGTCGTCGACCTCCACGCGATCACGGTTCCGCAGGACCCCGCCGAGCTGCGCGCCTCTAGAAGCGGC CGCG
TMP0054	P_{SVEN_4870} fwr	AATTCGCGGCCGCTTCTAGAGGATCGTCTCGCTCCGCTGACCCACCGGGAATGTTGAGCGGGGGGCGACGGTTGTT CCGTGCTA
	P_{SVEN_4870} rev	CTAGTAGCACGGAACAACCGTCGCCCCCCGCTCAACATTCCCGGTGGGTCAGCGGAGCGAGACGATCCTCTAGAAG CGGCCGCG
TMP0055	P_{SVEN_4793} fwr	AATTCGCGGCCGCTTCTAGAGGATCGGGGAGGAGTGCTTCGGCGTCTTCTCAGGTCGGCGGGTGAGCCGAAATCCG TGATA
	P_{SVEN_4793} rev	CTAGTATCACGGATTTCGGCTCACCCGCCGACCTGAGAAGACGCCGAAGCACTCCTCCCCGATCCTCTAGAAGCGG CCGCG
TMP0056	P_{SVEN_0063} fwr	AATTCGCGGCCGCTTCTAGAGCCGGCTCCATGTGACCCGGCTCACATGAACCGACGGTGCAGGCGGCGCGTGTGGG GCACTA
	P_{SVEN_0063} rev	CTAGTAGTGCCCCACACGCGCCGCCTGCACCGTCGGTTCATGTGAGCCGGGTCACATGGAGCCGGCTCTAGAAGCG GCCGCG
TMP0057	P_{SVEN_6501} fwr	AATTCGCGGCCGCTTCTAGAGGGCCGGTGGAACCGGGAGGAAACACCCATGCTGATCACCGGCCTCGTCGCGCTCG GAGTCCTGTA
	P_{SVEN_6501} rev	CTAGTACAGGACTCCGAGCGCGACGAGGCCGGTGATCAGCATGGGTGTTTCCTCCCGGTTCCACCGGCCCTCTAGA AGCGGCCGCG
TMP0058	P_{SVEN_3668} fwr	AATTCGCGGCCGCTTCTAGAGCGGCATGGGTGCCGCAAGGCGGTCTCGGGAATGTACGCCCCTTAGGATCCGTTGG GTGGGGTTA
	P_{SVEN_3668} rev	CTAGTAACCCCACCCAACGGATCCTAAGGGGCGTACATTCCCGAGACCGCCTTGCGGCACCCATGCCGCTCTAGAA GCGGCCGCG
TMP0059	P_{SVEN_2914} fwr	AATTCGCGGCCGCTTCTAGAGTCGTGGGGTGACACACGTCTGGTGGGTTGAAGGCGCCCTTCACCCCACCGTGTCC GTCTCTTCTA
	P_{SVEN_2914} rev	CTAGTAGAAGAGACGGACACGGTGGGGTGAAGGGCGCCTTCAACCCACCAGACGTGTGTCACCCCACGACTCTAGA AGCGGCCGCG
TMP0060	P_{SVEN_3369} fwr	AATTCGCGGCCGCTTCTAGAGCACCGTCGAAAAGGGTGACGCACGCGTACAACCCTGCCGGGGGGAAGCGTGTCCA ACATGCGTA
	P_{SVEN_3369} rev	CTAGTACGCATGTTGGACACGCTTCCCCCCGGCAGGGTTGTACGCGTGCGTCACCCTTTTCGACGGTGCTCTAGAA GCGGCCGCG
TMP0061	P_{SVEN_6611} fwr	AATTCGCGGCCGCTTCTAGAGCCCTTGGACCTTTGGCGACCCGCCTGGACAGCTCGACGAGCGGCCGCTTAGGGTC GGGGTCCGTA
	P_{SVEN_6611} rev	CTAGTACGGACCCCGACCCTAAGCGGCCGCTCGTCGAGCTGTCCAGGCGGGTCGCCAAAGGTCCAAGGGCTCTAGA AGCGGCCGCG
TMP0062	P_{SVEN_3215} fwr	AATTCGCGGCCGCTTCTAGAGGACGGCTGCCCCGCACAGCCCCGTGACAACCGCTCCGTAGCGTCATCGACGACAC GAGGTA
	P_{SVEN_3215} rev	CTAGTACCTCGTGTCGTCGATGACGCTACGGAGCGGTTGTCACGGGGCTGTGCGGGGCAGCCGTCCTCTAGAAGCG GCCGCG
TMP0063	P_{SVEN_3278} fwr	AATTCGCGGCCGCTTCTAGAGGGGCTGGCCCCGCCACACCACCCTCACACCCCTGACGCCGACCGACTCCGACCCA TCGCGATA
	P_{SVEN_3278} rev	CTAGTATCGCGATGGGTCGGAGTCGGTCGGCGTCAGGGGTGTGAGGGTGGTGTGGCGGGGCCAGCCCCTCTAGAAG CGGCCGCG
TMP0064	P_{SVEN_3293} fwr	AATTCGCGGCCGCTTCTAGAGCTGGCCGCGGGAGTCTGGCAGTCAGGCCTCGGACAGTTCATCGGCGGACTCGTCA TCGTCGCCTA
	P_{SVEN_3293} rev	CTAGTAGGCGACGATGACGAGTCCGCCGATGAACTGTCCGAGGCCTGACTGCCAGACTCCCGCGGCCAGCTCTAGA AGCGGCCGCG
TMP0065	P_{SVEN_3759} fwr	AATTCGCGGCCGCTTCTAGAGACCCTGAGGGTGTTCCCGGAGCGTCTCCACCCACAGGAGGTCGGGTCGTCCCCAC CCCTTA
	P_{SVEN_3759} rev	CTAGTAAGGGGTGGGGACGACCCGACCTCCTGTGGGTGGAGACGCTCCGGGAACACCCTCAGGGTCTCTAGAAGCG GCCGCG
TMP0066	P_{SVEN_4575} fwr	AATTCGCGGCCGCTTCTAGAGGAGGACGTCGAGTTCACGGCAGCGGGCCACGATCTCGGCGGCGAAGATCCCCTCC GCCACGAATA
	P_{SVEN_4575} rev	CTAGTATTCGTGGCGGAGGGGATCTTCGCCGCCGAGATCGTGGCCCGCTGCCGTGAACTCGACGTCCTCCTCTAGA AGCGGCCGCG
TMP0037	P_{SVEN_0136} fwr	AATTCGCGGCCGCTTCTAGAGCCATCGCCGCCGCTAGCGGGATCGAGGTCACCGGGGACGGCCGGATCGTCGTCGA CCGCACCTA
	P_{SVEN_0136} rev	CTAGTAGGTGCGGTCGACGACGATCCGGCCGTCCCCGGTGACCTCGATCCCGCTAGCGGCGGCGATGGCTCTAGAA GCGGCCGCG
TMP0038	P_{SVEN_0858} fwr	AATTCGCGGCCGCTTCTAGAGGCACCCGTCCATCCCAGCCGACGCGGGTCACCCTGTCCAGTTCCGGAAAGGGTCT TGAACTCCTA
	P_{SVEN_0858} rev	CTAGTAGGAGTTCAAGACCCTTTCCGGAACTGGACAGGGTGACCCGCGTCGGCTGGGATGGACGGGTGCCTCTAGA AGCGGCCGCG
TMP0039	P_{SVEN_3295} fwr	AATTCGCGGCCGCTTCTAGAGTTCTCATGTCCCTCCTCCCCCTGGCGGTCACATGGCGTGGTCGCCGTACACCTCA TTGACGCGTA
	P_{SVEN_3295} rev	CTAGTACGCGTCAATGAGGTGTACGGCGACCACGCCATGTGACCGCCAGGGGGAGGAGGGACATGAGAACTCTAGA AGCGGCCGCG

TMP0040	P_{SVEN_3475} fwr	AATTCGCGGCCGCTTCTAGAGCATCCCCGCCGCACCCGAGGGGCCCTGTCACCTTCTCGCGCCGGCATCCGTCATAGGTGCGTA
	P_{SVEN_3475} rev	CTAGTACGCACCTATGACGGATGCCGGCGCGAGAAGGTGACAGGGCCCCTCGGGTGCGGCGGGGATGCTCTAGAAGCGGCCGCG
TMP0041	P_{SVEN_3480} fwr	AATTCGCGGCCGCTTCTAGAGGGATCGTCGGCATCACCTGCCTGGAGGTCACCGCGGACGGCATCGCCGCGGTCCGCAGCCAGTA
	P_{SVEN_3480} rev	CTAGTACTGGCTGCGGACCGCGGCGATGCCGTCCGCGGTGACCTCCAGGCAGGTGATGCCGACGATCCCTCTAGAAGCGGCCGCG
TMP0042	P_{SVEN_3821} fwr	AATTCGCGGCCGCTTCTAGAGAGGTCGGGTTGGGCCGGGCCGGGCCGGTCACGTCGGTCCGGGCCGGTCACGTCAGGCCCCTCTA
	P_{SVEN_3821} rev	CTAGTAGAGGGGCCTGACGTGACCGGCCCGGACCGACGTGACCGGCCCGGCCCGGCCCAACCCGACCTCTCTAGAAGCGGCCGCG
TMP0043	P_{SVEN_3859} fwr	AATTCGCGGCCGCTTCTAGAGCCCCCGCAACGGGGGTGACAGACGGTGTCACATCGGCGAGGTTTGAACCGTCATGGAGCCATA
	P_{SVEN_3859} rev	CTAGTATGGCTCCATGACGGTTCAAACCTCGCCGATGTGACACCGTCTGTCACCCCCGTTGCGGGGGCTCTAGAAGCGGCCGCG
TMP0044	P_{SVEN_1176} fwr	AATTCGCGGCCGCTTCTAGAGTCTTCCCCGGCCCGTCCGCCGCCGCTGTCACATCACCGTGGGTCCCCGCGTCAAGGCGGTGTA
	P_{SVEN_1176} rev	CTAGTACACCGCCTTGACGCGGGGACCCACGGTGATGTGACAGCGGCGGCGGACGGGCCGGGGAAGACTCTAGAAGCGGCCGCG
TMP0046	P_{SVEN_4377} fwr	AATTCGCGGCCGCTTCTAGAGAACTTTCGAAGATCGCCGTCGGGGATGTCGAGGACGCCCCGCCGGCTCCGACCGAGGGGTGTA
	P_{SVEN_4377} rev	CTAGTACACCCCTCGGTCGGAGCCGGCGGGGCGTCCTCGACATCCCCGACGGCGATCTTCGAAAGTTCTCTAGAAGCGGCCGCG
TMP0047	P_{SVEN_7131} fwr	AATTCGCGGCCGCTTCTAGAGTCCCTGTCACATCGCCCGATCGACGTGTCAGCGAGCACCGCACACCACGAACCCCGGTA
	P_{SVEN_7131} rev	CTAGTACCGGGGTTCGTGGTGTGCGGTGCTCGCTGACACGTCGATCGGGCGATGTGACAGGGACTCTAGAAGCGGCCGCG
TMP0048	P_{SVEN_0980} fwr	AATTCGCGGCCGCTTCTAGAGTGTTCCTCGAAGCCTGGCGCTGTCGCGGGAAGGTGCACGCCGAGGGCGGCAGTCTGCGGCTA
	P_{SVEN_0980} rev	CTAGTAGCCGCAGACTGCCGCCCTCGGCGTGCACCTTCCCGCGACAGCGCCAGGCTTCGAGGAACACTCTAGAAGCGGCCGCG
TMP0067	P_{SVEN_0015} fwr	AATTCGCGGCCGCTTCTAGAGGGAGCACCTGCCGGGCAGCGCTCTGCGGGACCTGCGGCGCTTCCAGTGGGACTTCGCCACTA
	P_{SVEN_0015} rev	CTAGTAGTGGCGAAGTCCCACTGGAAGCGCCGCAGGTCCCGCAGAGCGCTGCCCGGCAGGTGCTCCCTCTAGAAGCGGCCGCG
TMP0049	P_{SVEN_3871} fwr	AATTCGCGGCCGCTTCTAGAGCTCTGTGGCAGGCTTGGCCGGTGTTCGGGTCTGAGCATGCGTACGGGGGCTTCCGCGATA
	P_{SVEN_3871} rev	CTAGTATCGCGGAAGCCCCCGTACGCATGCTCAGACCCGAACACCGGCCAAGCCTGCCACAGAGCTCTAGAAGCGGCCGCG
TMP0050	P_{SVEN_0434} fwr	AATTCGCGGCCGCTTCTAGAGCCGATCGTCGATCACCCGGATAAAGTGTTATCCCTCCCGCGCCCACGGGTCTCCGAACGACGTA
	P_{SVEN_0434} rev	CTAGTACGTCGTTCGGAGACCCGTGGGCGCGGGAGGGATAACACTTTATCCGGGTGATCGACGATCGGCTCTAGAAGCGGCCGCG
TMP0051	P_{SVEN_6745} fwr	AATTCGCGGCCGCTTCTAGAGCGTCGTATTCTTTGCCGACGCAGAGGCCGGTCGCCGTCCGCCGGTGGACCGCCTCCCTGGAGAGTA
	P_{SVEN_6745} rev	CTAGTACTCTCCAGGGAGGCGGTCCACCGGCGGACGGCGACCGGCCTCTGCGTCGGCAAAGAATACGACGCTCTAGAAGCGGCCGCG
TMP0052	P_{SVEN_4562} fwr	AATTCGCGGCCGCTTCTAGAGCGAGCCGGACCATGGCCCGGGAGAGCGTCGACTGGGGCACGCCCATCTCGGCGGCGGCCCGGTA
	P_{SVEN_4562} rev	CTAGTACCGGGCCGCCGCCGAGATGGGCGTGCCCCAGTCGACGCTCTCCCGGGCCATGGTCCGGCTCGCTCTAGAAGCGGCCGCG
TMP0102	P_{SVEN_3185} fwr	AATTCGCGGCCGCTTCTAGAGGAGTGCCGAAGGGTGCCGTCCGACCCGTAACTCTTTCGAGTGACCGTCGTTGAGAGTGCTA
	P_{SVEN_3185} rev	CTAGTAGCACTCTCAACGACGGTCACTCGAAAGAGTTACGGGTCGGACGGCACCCTTCGGCACTCCTCTAGAAGCGGCCGCG
TMP0036	P_{SVEN_4540} fwr	AATTCGCGGCCGCTTCTAGAGGGTCGCCACCCCCCACAGGAGAGACCCCGGCCGTCGTCCACGGAGCCGCAGCACGGCTCCGTACTA
	P_{SVEN_4540} rev	CTAGTAGTACGGAGCCGTGCTGCGGCTCCGTGGACGACGGCCGGGGTCTCTCCTGTGGGGGGTGGCGACCCTCTAGAAGCGGCCGCG
TMP0074	$P_{SMb21484}$ fwr	AATTCGCGGCCGCTTCTAGAGCTCAACTGGATGTCCCTAGACCACTCAAACTGGTGATGTCGCTTTTGGTTCCCGTGGGCTA
	$P_{SMb21484}$ rev	CTAGTAGCCCACGGGAACCAAAAGCGACATCACCAGTTTGAGTGGTCTAGGGACATCCAGTTGAGCTCTAGAAGCGGCCGCG
TMP0075	P_{SM_b20531} fwr	AATTCGCGGCCGCTTCTAGAGGGCAAAACATTTGCCGCGCGGACATGTAACAAGTAGCGAAACTCGGCGAATTGGGAGGATA
	P_{SM_b20531} rev	CTAGTATCCTCCCAATTCGCCGAGTTTCGCTACTTGTTACATGTCCGCGCGGCAAATGTTTTGCCCTCTAGAAGCGGCCGCG
TMP0076	$P_{SMa0143}$ fwr	AATTCGCGGCCGCTTCTAGAGAAACTCCGCAATTTGGCTAGAAGAGGGAATAGACCGACGACTCAGCCGTTCTGACACAATTA
	$P_{SMa0143}$ rev	CTAGTAATTGTGTCAGAACGGCTGAGTCGTCGGTCTATTCCCTCTTCTAGCCAAATTGCGGAGTTTCTCTAGAAGCGGCCGCG
TMP0078	$P_{SMc02713}$ fwr	AATTCGCGGCCGCTTCTAGAGGAACATTTGGTCCTAAGTCTGCAAGGGAAGAGCCGGAACGGAAAGAGGTTTTTGCGCCCCTA
	$P_{SMc02713}$ rev	CTAGTAGGGGCGCAAAAACCTCTTTCCGTTCCGGCTCTTCCCTTGCAGACTTAGGACCAAATGTTCCTCTAGAAGCGGCCGCG

TMP0079	$P_{SMc04051}$ fwr	AATTCGCGGCCGCTTCTAGAGATCGCCAGCGGACGTAGCGCATCATGGAATAAGCGAGGCAGCTCGCTCGTCTCTA CGCCGCTA
	$P_{SMc04051}$ rev	CTAGTAGCGGCGTAGAGACGAGCGAGCTGCCTCGCTTATTCCATGATGCGCTACGTCCGCTGGCGATCTCTAGAAG CGGCCGCG
TMP0080	$P_{SMb20592}$ fwr	AATTCGCGGCCGCTTCTAGAGATCCGAAACTTGGCCGGCACATAGCTGGGAACATTTCCGGAGATAGGGCATCCAA TATCCGATA
	$P_{SMb20592}$ rev	CTAGTATCGGATATTGGATGCCCTATCTCCGGAAATGTTCCCAGCTATGTGCCGGCCAAGTTTCGGATCTCTAGAA GCGGCCGCG
TMP0081	P_{SM_b20030} fwr	AATTCGCGGCCGCTTCTAGAGGCGTCGACAAAAAAATTCGCATCCATGTCACACCGGCGGCCGCTGTCTCGTCATG GTGTCGTA
	P_{SM_b20030} rev	CTAGTACGACACCATGACGAGACAGCGGCCGCCGGTGTGACATGGATGCGAATTTTTTTGTCGACGCCTCTAGAAG CGGCCGCG
TMP0082	$P_{SMc01150}$ fwr	AATTCGCGGCCGCTTCTAGAGTGTTGAGCGTTTTTTTCGCCCCGCTTGTCGGCTATCAATAGCGCCATTCGTCTTC AGACCATA
	$P_{SMc01150}$ rev	CTAGTATGGTCTGAAGACGAATGGCGCTATTGATAGCCGACAAGCGGGGCGAAAAAAACGCTCAACACTCTAGAAG CGGCCGCG
TMP0071	$P_{ECDH10B\_2741}$ fwr	AATTCGCGGCCGCTTCTAGAGGACAAACAAAAACAGATGCGTTACGGAACTTTACAAAAACGAGACACTCTAACCC TTTGTA
	$P_{ECDH10B\_2741}$ rev	CTAGTACAAAGGGTTAGAGTGTCTCGTTTTTGTAAAGTTCCGTAACGCATCTGTTTTTGTTTGTCCTCTAGAAGCG GCCGCG
TMP0072	$P_{ECDH10B\_4491}$ fwr	AATTCGCGGCCGCTTCTAGAGTTTTATACCTACCTTATAACACTTAGAAAAACAACATGTTAAAAATGTCTATTGG AATA
	$P_{ECDH10B\_4491}$ rev	CTAGTATTCCAATAGACATTTTTAACATGTTGTTTTTCTAAGTGTTATAAGGTAGGTATAAAACTCTAGAAGCGGC CGCG
TMP0020	$P_{BL04030\ -51\ to\ +8}$ fwr	AATTCGCGGCCGCTTCTAGAGATAAAAAAACCCGTATCAAATCGGCGGAGCCAGCCGTTTATTAAGTAAGAGGCCT CTTTTA
	$P_{BL04030\ -51\ to\ +8}$ rev	CTAGTAAAAGAGGCCTCTTACTTAATAAACGGCTGGCTCCGCCGATTTGATACGGGTTTTTTTATCTCTAGAAGCG GCCGCG
TMP0021	$P_{BL04030\ -36\ to\ +8}$ fwr	AATTCGCGGCCGCTTCTAGAGTCAAATCGGCGGAGCCAGCCGTTTATTAAGTAAGAGGCCTCTTTTA
	$P_{BL04030\ -36\ to\ +8}$ rev	CTAGTAAAAGAGGCCTCTTACTTAATAAACGGCTGGCTCCGCCGATTTGACTCTAGAAGCGGCCGCG
TMP0022	$P_{BL04030\ -21\ to\ +8}$ fwr	AATTCGCGGCCGCTTCTAGAGCAGCCGTTTATTAAGTAAGAGGCCTCTTTTA
	$P_{BL04030\ -21\ to\ +8}$ rev	CTAGTAAAAGAGGCCTCTTACTTAATAAACGGCTGCTCTAGAAGCGGCCGCG
TMP0023	$P_{BL04030\ -66\ to\ -8}$ fwr	AATTCGCGGCCGCTTCTAGAGTTTTTTGTTACAATCATAAAAAAAACCCGTATCAAATCGGCGGAGCCAGCCGTTTA TTAATA
	$P_{BL04030\ -66\ to\ -8}$ rev	CTAGTATTAATAAACGGCTGGCTCCGCCGATTTGATACGGGTTTTTTTATGATTGTAACAAAAAACTCTAGAAGCG GCCGCG
TMP0024	$P_{BL04030\ -66\ to\ -23}$ fwr	AATTCGCGGCCGCTTCTAGAGTTTTTTGTTACAATCATAAAAAAAACCCGTATCAAATCGGCGGAGTA
	$P_{BL04030\ -66\ to\ -23}$ rev	CTAGTACTCCGCCGATTTGATACGGGTTTTTTTATGATTGTAACAAAAAACTCTAGAAGCGGCCGCG
TMP0025	$P_{BL04030\ -66\ to\ -38}$ fwr	AATTCGCGGCCGCTTCTAGAGTTTTTTGTTACAATCATAAAAAAAACCCGTTA
	$P_{BL04030\ -66\ to\ -38}$ rev	CTAGTAACGGGTTTTTTTATGATTGTAACAAAAAACTCTAGAAGCGGCCGCG
TMP0026	$P_{BL04030\ -51\ to\ +8}$ fwr	AATTCGCGGCCGCTTCTAGAGATAAAAAAAACCCGTATCAAATCGGCGGAGCCAGCCGTTTATTAATA
	$P_{BL04030\ -51\ to\ +8}$ rev	CTAGTATTAATAAACGGCTGGCTCCGCCGATTTGATACGGGTTTTTTTATCTCTAGAAGCGGCCGCG
TMP0027	$P_{BL04030\ -36\ to\ +8}$ fwr	AATTCGCGGCCGCTTCTAGAGTCAAATCGGCGGAGCCAGCCGTTTATTAATA
	$P_{BL04030\ -36\ to\ +8}$ rev	CTAGTATTAATAAACGGCTGGCTCCGCCGATTTGACTCTAGAAGCGGCCGCG
TMP0099	$P_{ecf105\ -55\ to\ +1}$ fwr	AATTCGCGGCCGCTTCTAGAGAATATATTATTCTTTTTTTACAAAATGTGTAGGGTGACTTATCATTCTTTACGTC TTA
	$P_{ecf105\ -55\ to\ +1}$ rev	CTAGTAAGACGTAAAGAATGATAAGTCACCCTACACATTTTGTAAAAAAAGAATAATATATTCTCTAGAAGCGGCC GCG
TMP0100	$P_{ecf105\ -30\ to\ +1}$ fwr	AATTCGCGGCCGCTTCTAGAGTGTGTAGGGTGACTTATCATTCTTTACGTCTTA
	$P_{ecf105\ -30\ to\ +1}$ rev	CTAGTAAGACGTAAAGAATGATAAGTCACCCTACACACTCTAGAAGCGGCCGCG
TMP0101	$P_{SVEN\_0399\ -35\ to\ +1}$ fwr	AATTCGCGGCCGCTTCTAGAGCCCATCCGCAGGGCCGTCCGCTACGAAGAACGGGCGTA
	$P_{SVEN\_0399\ -35\ to\ +1}$ rev	CTAGTACGCCCGTTCTTCGTAGCGGACGGCCCTGCGGATGGGCTCTAGAAGCGGCCGCG

*Putative -35 and -10 promoter elements are underlined.

V. ECF switches from *Escherichia coli*, *Sinorhizobium meliloti* and *Streptomyces venezuelae*

V.1 Codon adjustment table

The codon usage table was generated using the codon usage frequency a subset of predicted highly expressed genes previously identified (Karlin et al., 2001). Codon adjustment was performed by substitution of a given codon for the one used with similar frequency in *B. subtilis*.

Table S5. Genes used to generate the codon usage table, Figure 1.

Gene product function	Gene product	*B. subtilis* locus tag	*S. meliloti* locus tag	*S. venezuelae* locus tag
Ribosomal	ribosomal protein S1	BSU22880	SM2011_c00335	SVEN_1623
	ribosomal protein S2	BSU16490	SM2011_c02101	SVEN_5303
	ribosomal protein S3	BSU01220	SM2011_c01303	SVEN_4385
	ribosomal protein S4	BSU29660	SM2011_c00485	SVEN_1106
	ribosomal protein S5	BSU01330	SM2011_c01292	SVEN_4396
	ribosomal protein S9	BSU01500	SM2011_c01803	SVEN_4413
	ribosomal protein S13	BSU01410	SM2011_c01287	SVEN_4405
	ribosomal protein L1	BSU01030	SM2011_c01320	SVEN_4341
	ribosomal protein L3	BSU01160	SM2011_c01309	SVEN_4379
	ribosomal protein L2	BSU01190	SM2011_c01306	SVEN_4382
	ribosomal protein L4	BSU01170	SM2011_c01308	SVEN_4380
	ribosomal protein L5	BSU01280	SM2011_c01297	SVEN_4391
	ribosomal protein L11	BSU01020	SM2011_c01321	SVEN_4340
	ribosomal protein L13	BSU01490	SM2011_c01804	SVEN_4412
	ribosomal protein L14	BSU01260	SM2011_c01299	SVEN_4389
	ribosomal protein L16	BSU01230	SM2011_c01302	SVEN_4386
	ribosomal protein L17	BSU01440	SM2011_c01283	SVEN_4408
	ribosomal protein L20	BSU28850	SM2011_c00364	SVEN_1193
Chaperone	heat shock protein 70	BSU25470	SM2011_c02857	SVEN_3433
Translation/transcription	elongation factor Ts	BSU16500	SM2011_c02100	SVEN_5304
	DNA-directed RNA polymerase beta	BSU01070	SM2011_c01317	SVEN_4345
	DNA-directed RNA polymerase beta'	BSU01080	SM2011_c01316	SVEN_4346
	ATP-dependent RNA helicase	BSU04580	SM2011_c01090	SVEN_4812
Energy metabolism	phosphoglycerate kinase	BSU33930	SM2011_c03981	SVEN_1575
	pyruvate dehydrogenase E1 beta	BSU14590	SM2011_c01031	SVEN_3586
	ATP synthase F1 alpha	BSU36830	SM2011_c02499	SVEN_5023
	ATP synthase F1 beta	BSU36810	SM2011_c02501	SVEN_5025
Nucleotide or amino acid biosynthesis	ketol-acid reductoisomerase	BSU28290	SM2011_c04346	SVEN_5190
Other	GTP-binding protein	BSU14770	SM2011_c03242	SVEN_4758

Table S6. Codon usage table, Related to Figure 1.

Amino acid	Codon	*B. subtilis* usage frequency	*S. meliloti* usage frequency	*S. venezuelae* usage frequency
Alanine	GCT	0.38	0.11	0.06
	GCA	0.29	0.12	0.01
	GCG	0.23	0.30	0.31
	GCC	0.10	0.47	0.62
Arginine	CGT	0.58	0.23	0.30
	CGC	0.32	0.68	0.59
	AGA	0.08	0.01	0.00
	CGA	0.02	0.00	0.01
	CGG	0.01	0.07	0.09
	AGG	0.00	0.01	0.01
Asparagine	AAC	0.74	0.84	0.99
	AAT	0.26	0.16	0.01
Aspartate	GAT	0.56	0.25	0.01
	GAC	0.44	0.75	0.99
Cysteine	TGT	0.65	0.02	0.14
	TGC	0.35	0.98	0.86
Glutamine	CAA	0.65	0.02	0.00
	CAG	0.35	0.98	1.00
Glutamate	GAA	0.75	0.53	0.03
	GAG	0.25	0.47	0.97
Glycine	GGT	0.39	0.21	0.31
	GGA	0.30	0.03	0.02
	GGC	0.27	0.74	0.65
	GGG	0.03	0.02	0.02
Histidine	CAC	0.59	0.64	0.99
	CAT	0.41	0.36	0.01
Isoleucine	ATC	0.60	0.89	0.99
	ATT	0.40	0.11	0.01
Leucine	CTT	0.50	0.13	0.02
	TTA	0.19	0.00	0.00
	CTG	0.11	0.42	0.50
	TTG	0.10	0.03	0.00
	CTC	0.05	0.43	0.48
	CTA	0.05	0.00	0.00
Lysine	AAA	0.83	0.06	0.00
	AAG	0.17	0.94	1.00
Methionine	ATG	0.96	0.99	1.00
	ATA	0.04	0.06	0.00
Phenylalanine	TTC	0.69	0.94	0.99
	TTT	0.31	0.06	0.01
Proline	CCT	0.43	0.06	0.02
	CCG	0.28	0.80	0.69
	CCA	0.28	0.01	0.00
	CCC	0.01	0.14	0.30
Serine	TCT	0.45	0.04	0.01
	TCA	0.26	0.01	0.00
	AGC	0.13	0.12	0.11
	TCC	0.08	0.37	0.47
	AGT	0.07	0.01	0.00
	TCG	0.01	0.46	0.40
Threonine	ACA	0.47	0.03	0.00
	ACT	0.35	0.03	0.01
	ACG	0.15	0.40	0.28
	ACC	0.03	0.54	0.70
Tryptophan	TGG	1.00	1.00	1.00
Tyrosine	TAC	0.61	0.66	1.00
	TAT	0.39	0.34	0.00
Valine	GTT	0.43	0.17	0.06
	GTA	0.33	0.04	0.00
	GTG	0.12	0.19	0.22
	GTC	0.12	0.59	0.72

V.2 ECF group distribution

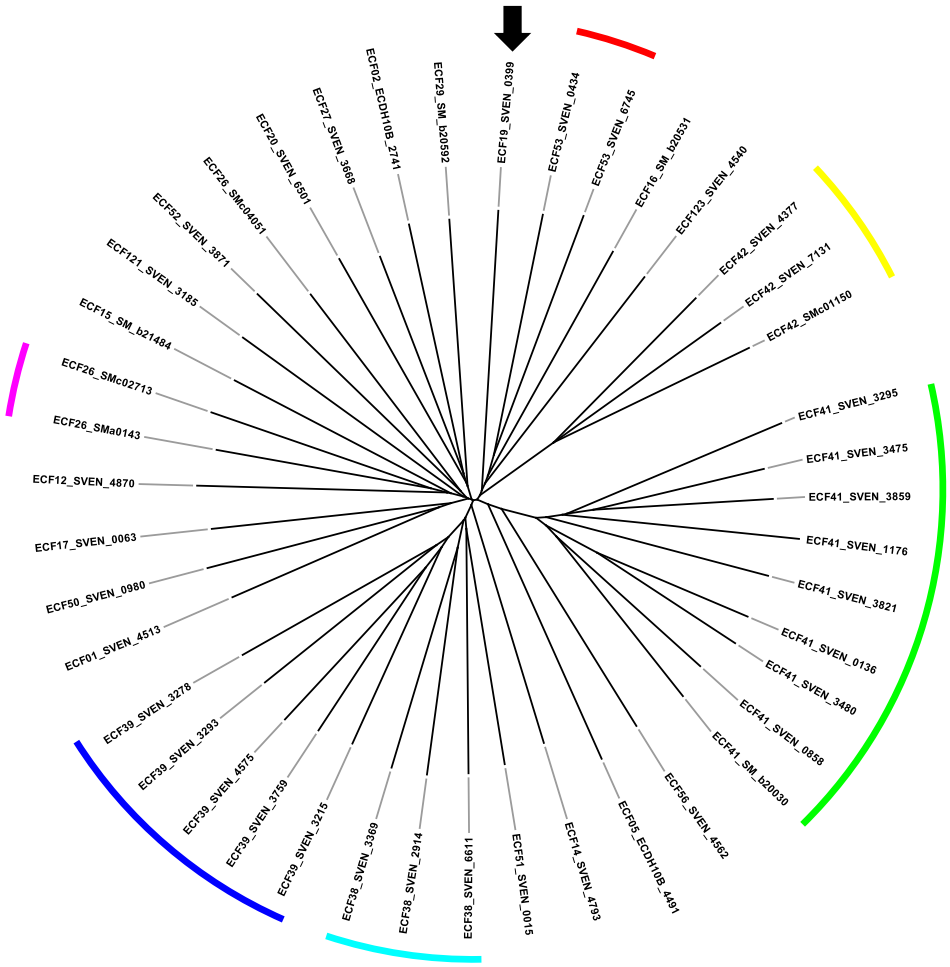

Figure S2. *Escherichia coli*, *Sinorhizobium meliloti* and *Streptomyces venezuelae* ECF library represented as a phylogenetic tree build with their full-length protein sequences, Related to Figure 1. Members are labeled with the ECF group number and the locus. Groups represented by more than one protein are highlighted: green, ECF41; yellow, ECF42; red, ECF53; pink, ECF26; dark blue, ECF39; and light blue, ECF38. The black arrow indicates the only ECF of this library that produced and active switch (see **Figure S3**).

V.3 Activity of ECF-based switches

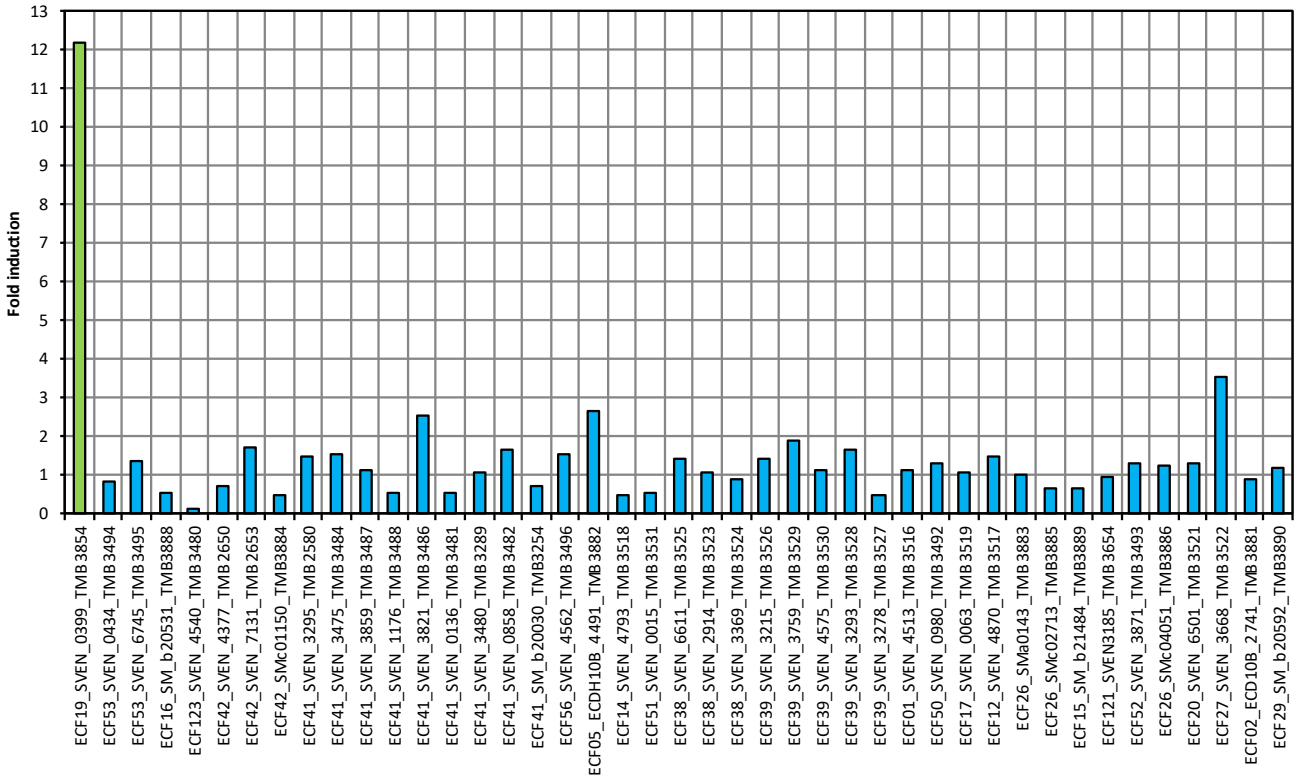

Figure S3. Fold induction of ECF-based switches, Related to Figure 1. Each switch is represented by its ECF group, the locus tag and the strain name. Strains were grown at 37°C and in chemically defined MCSE medium (Radeck et al., 2013) to exponential phase. Induction of ECF expression was accomplished through the medium supplementation with 0.5% xylose (for strains in which expression of the ECF coding gene was dependent on P_{xylA}) or 10 µg/mL of bacitracin (for strains in wish expression of the ECF coding gene was dependent on P_{lial}, i.e., TMB3254 and TMB3289). Luminescence measurements were performed and in a microtiter plate reader and the fold induction value plotted here refers to the ration between the output of induced and un-induced samples 1 hour after induction. The SVEN_0399 switch (ECF19_SVEN_0399_TMB3854) is shown in green as an example of an active switch.

VI. Promoters

VI.1 Promoter list and sequence

All promoters are listed in Table S7.

VI.2 Promoter behavior

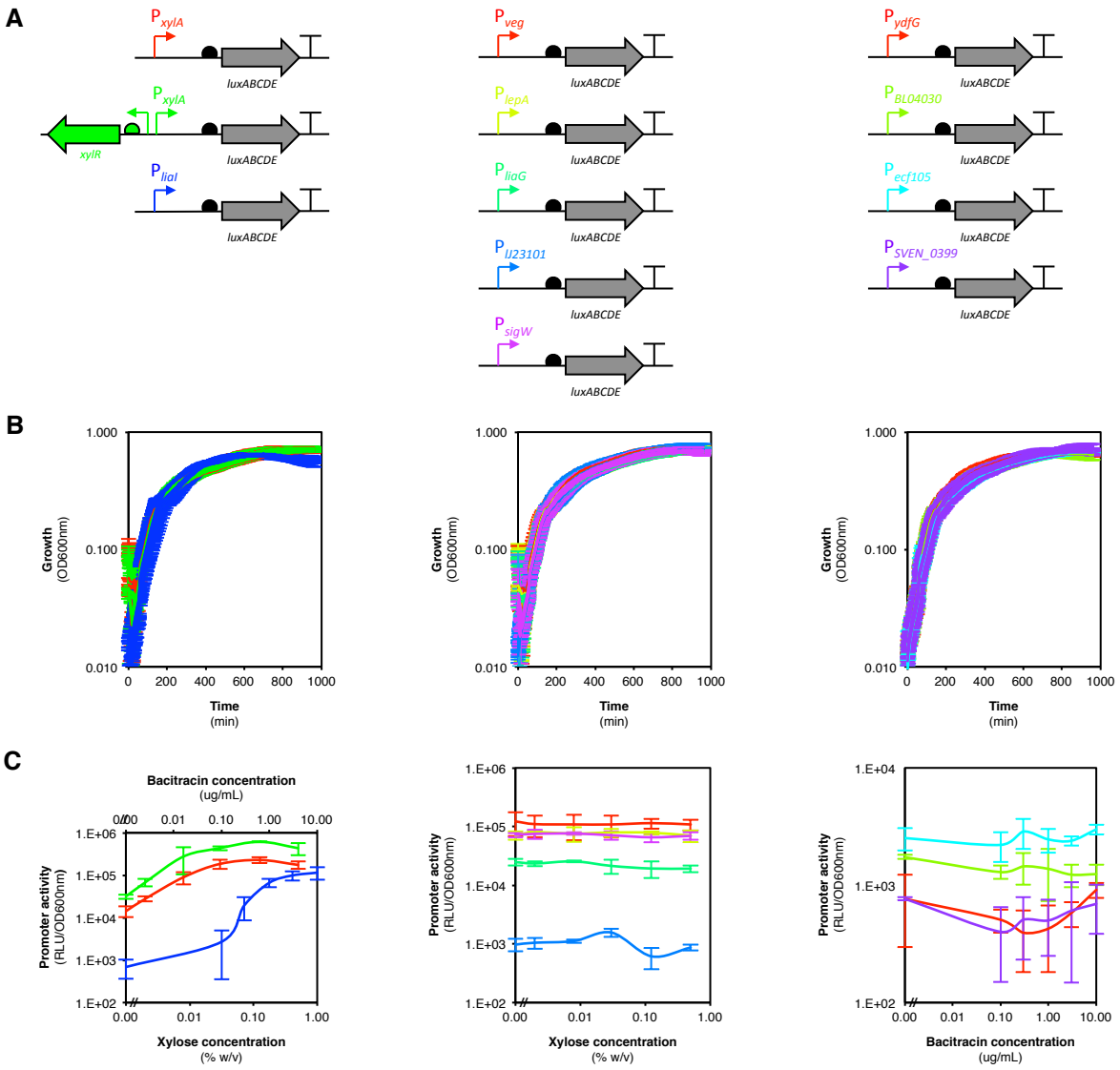

Figure S4. Behavior of the promoters used in this study, Related to Figure 1 and Figure 2. Promoters P_{xylA} with and without the regulator XylR and P_{liaI} are inducible by xylose or bacitracin, respectively. Promoters P_{veg}, P_{lepA}, P_{liaG}, P_{J23101} and P_{sigW} were used for antisense transcription experiments. Promoter P_{ydfG}, $P_{BL04030}$, P_{ecf105} and P_{SVEN_0399} are ECF target promoters used in the switches. **A.** Genetic layout of promoter-reporter constructs. Thick arrows represent open reading frames. 'T' represent terminators. Half circles represent ribosome binding sites. Thin arrows represent promoters. **B.** Growth curves of the strains containing each of the constructs represented in panel A. Each strain is represented in the same color used to represent the promoter in panel A. The inducer was added to the growing culture after 60 minutes. Vertical bars represent standard deviations of three independent experiments. Source data can be found in Additional File 3. **C.** Dose-response curves drawn using the relative luminescence units (RLU) normalized by the optical density measured at 600 nm (OD600nm) value achieved 90 min after the addition of inducer. Final concentrations of xylose used for induction were 0, 0.002, 0.008, 0.03, 0.125 or 0.5 % (w/v) while final concentrations of bacitracin used for induction were 0, 0.1, 0.3, 1, 3 or 10 μg/ml. Vertical bars represent standard deviations of three independent experiments. Source data can be found in Additional File 3.

VI.3 Increased basal level of BL00106-target promoter

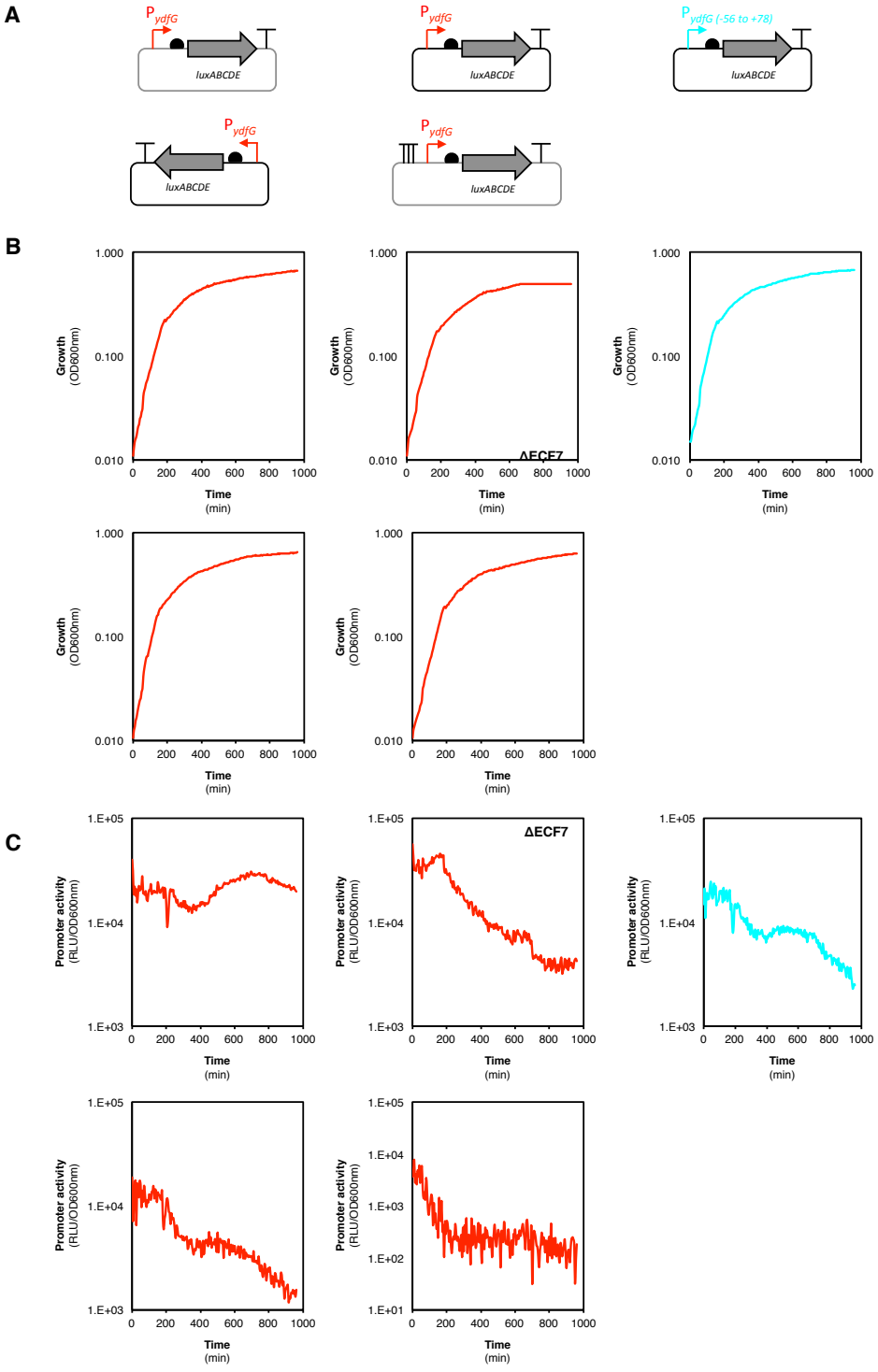

Figure S5. Behavior of the P_{ydfG} promoter in the absence of BL00106, Related to Figure 2. **A.** Genetic layout of promoter-reporter constructs. Thick arrows represent open reading frames. 'T' represent terminators. Half circles represent ribosome binding sites. Thin arrows represent promoters. **B.** Growth curves of the strains containing each of the constructs represented in panel A, in the same order. Source data can be found in Additional File 3. **C.** Luminescence output represented through relative luminescence units (RLU) normalized by the optical density measured at 600 nm (OD600nm). Source data can be found in Additional File 3.

VII. ECF switch behavior

VII.1 Behavior upon variation of the ECF-promoter pair.

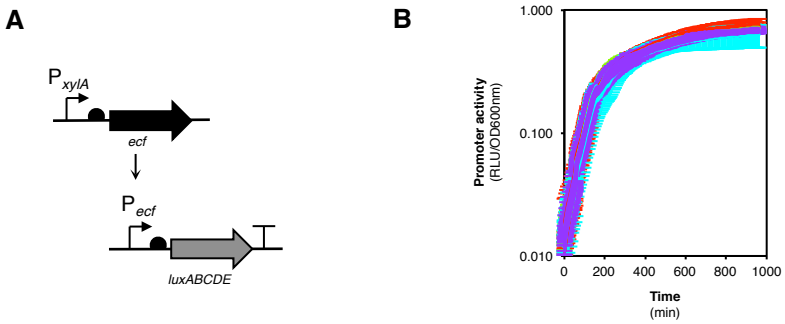

Figure S6. Behavior of the ECF switch upon variation of the ECF-promoter pair, Related to Figure 1. **A.** Genetic layout of promoter-reporter constructs is depicted on the left side of the panel. Thick arrows represent open reading frames. 'T' represents terminators. Half circles represent ribosome binding sites. Thin arrows represent promoters. **B.** Growth curves of the strains containing each of the ECF-promoter constructs. BL00106, red; BL04030, green; ECF105, light blue; SVEN_0399, purple. The inducer was added to the growing culture after 60 minutes. Final concentrations of xylose used for induction were 0, 0.002, 0.008, 0.03, 0.125 or 0.5% (w/v). Vertical bars represent standard deviations of three independent experiments. Source data can be found in Additional File 3.

VII.2 Behavior upon alteration of copy number of each module

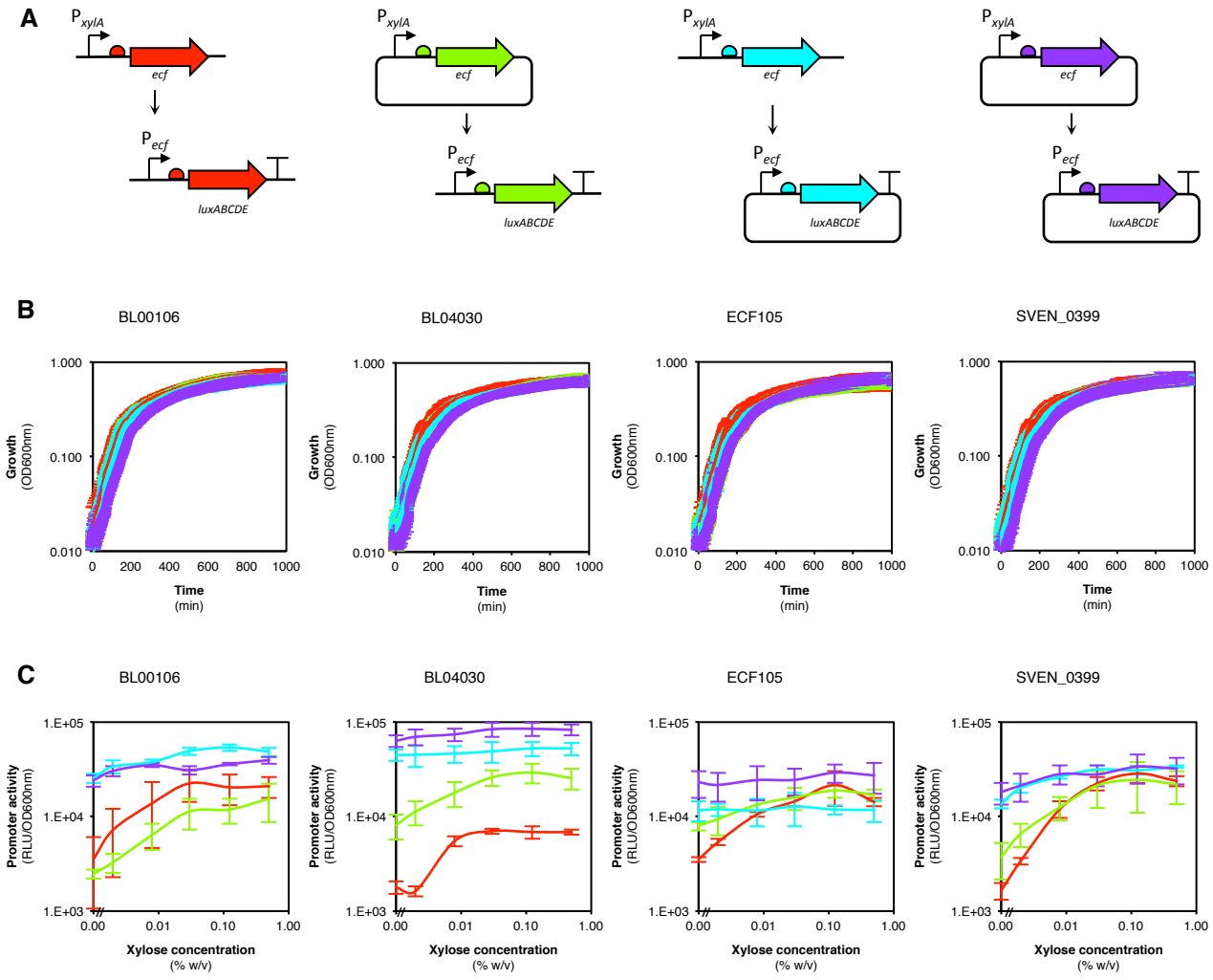

Figure S7. Behavior of the ECF switch upon alteration of the copy number of each module, Related to Figure 2. **A.** Genetic layout of promoter-reporter constructs. Thick arrows represent open reading frames. 'T' represent terminators. Half circles represent ribosome binding sites. Thin arrows represent promoters. **B.** Growth curves of the strains containing each of the constructs represented in panel A, represented using the same color code. The inducer was added to the growing culture after 60 minutes. Final concentrations of xylose used for induction were 0, 0.002, 0.008, 0.03, 0.125 or 0.5 % (w/v). Vertical bars represent standard deviations of three independent experiments. Source data can be found in Additional File 3. **C.** Dose-response curves drawn using the luminescence output value, represented through relative luminescence units (RLU) normalized by the optical density measured at 600 nm (OD600nm), achieved 90 min after the addition of the inducer to the exponentially growing culture. Each graph represents the measurements performed with the *B. subtilis* strain harboring the switches depicted in panel A and are color coded accordingly. Final concentrations of xylose used for induction were 0, 0.002, 0.008, 0.03, 0.125 or 0.5 % (w/v). Vertical bars represent standard deviations calculated from three independent experiments. Source data can be found in Additional File 3.

VII.3 Behavior upon alteration of the inducible promoter

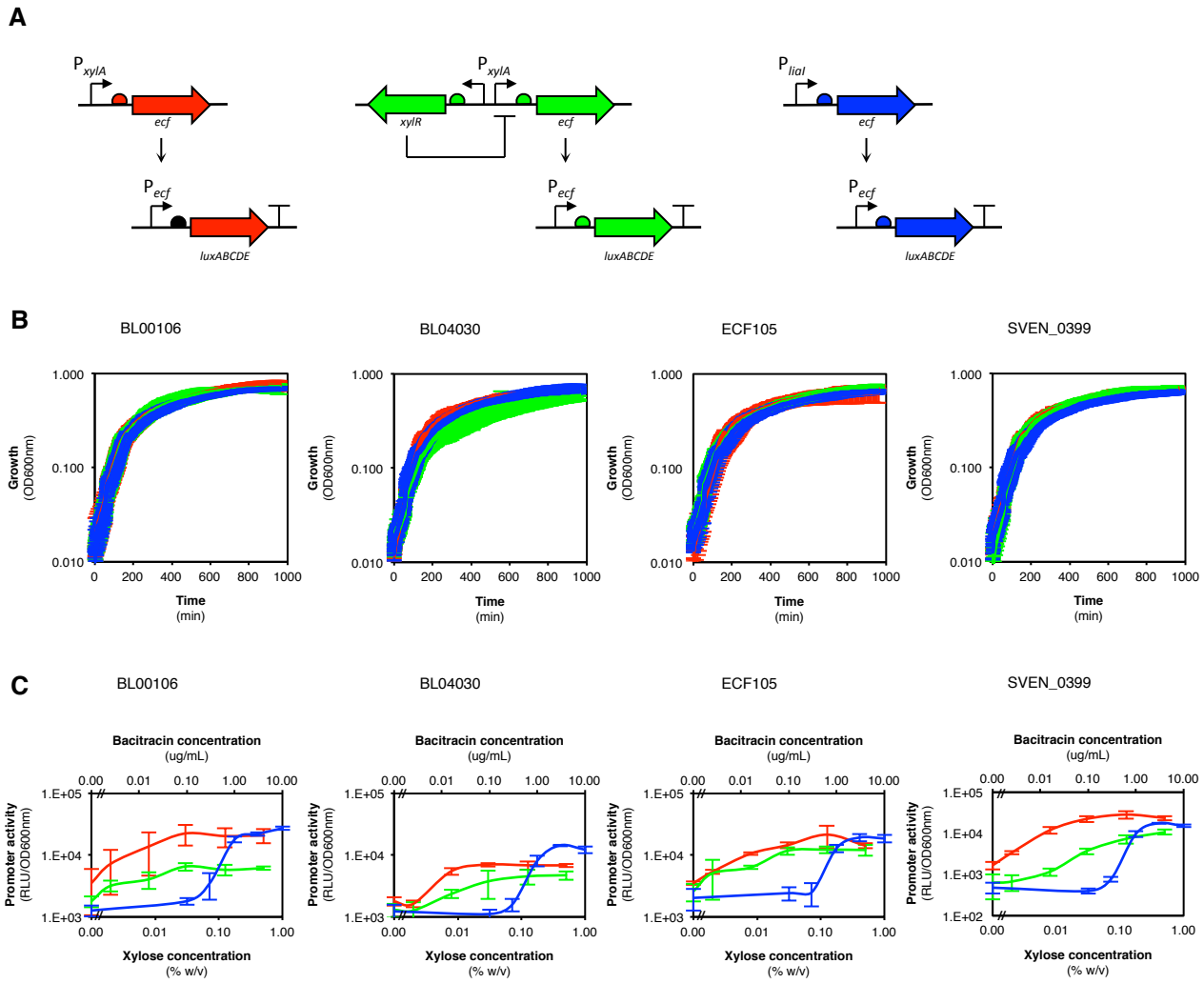

Figure S8. Behavior of the ECF switch upon alteration of the inducible promoter, Related to Figure 2. **A.** Genetic layout of promoter-reporter constructs. Thick arrows represent open reading frames. 'T' represents terminators. Half circles represent ribosome binding sites. Thin arrows represent promoters. An arrow with a 'T' end represents repression. **B.** Growth curves of the strains containing each of the constructs represented in panel A represented using the same color code. The inducer was added to the growing culture after 60 minutes. Final concentrations of xylose used for induction were 0, 0.002, 0.008, 0.03, 0.125 or 0.5 % (w/v) while final concentrations of bacitracin used for induction of promoter P_{lial} were 0, 0.1, 0.3, 1, 3 or 10 μg/ml. Vertical bars represent standard deviations of three independent experiments. Source data can be found in Additional File 3. **C.** Dose-response curves drawn using the luminescence output value, represented through relative luminescence units (RLU) normalized by the optical density measured at 600 nm (OD600nm), achieved 90 min after the addition of the inducer to the exponentially growing culture. Each graph represents the measurements performed with the *B. subtilis* strain harboring the switch depicted in panels A and are color coded accordingly. Final concentrations of xylose used for induction of P_{xylA} were 0, 0.002, 0.008, 0.03, 0.125 or 0.5 % (w/v) while final concentration of bacitracin used for induction of P_{lial} were 0, 0.1, 0.3, 1, 3 or 10 μg/ml. Vertical bars represent standard deviations calculated from three independent experiments. Source data can be found in Additional File 3.

VII.4 Behavior upon addition of ssrA-tag variants

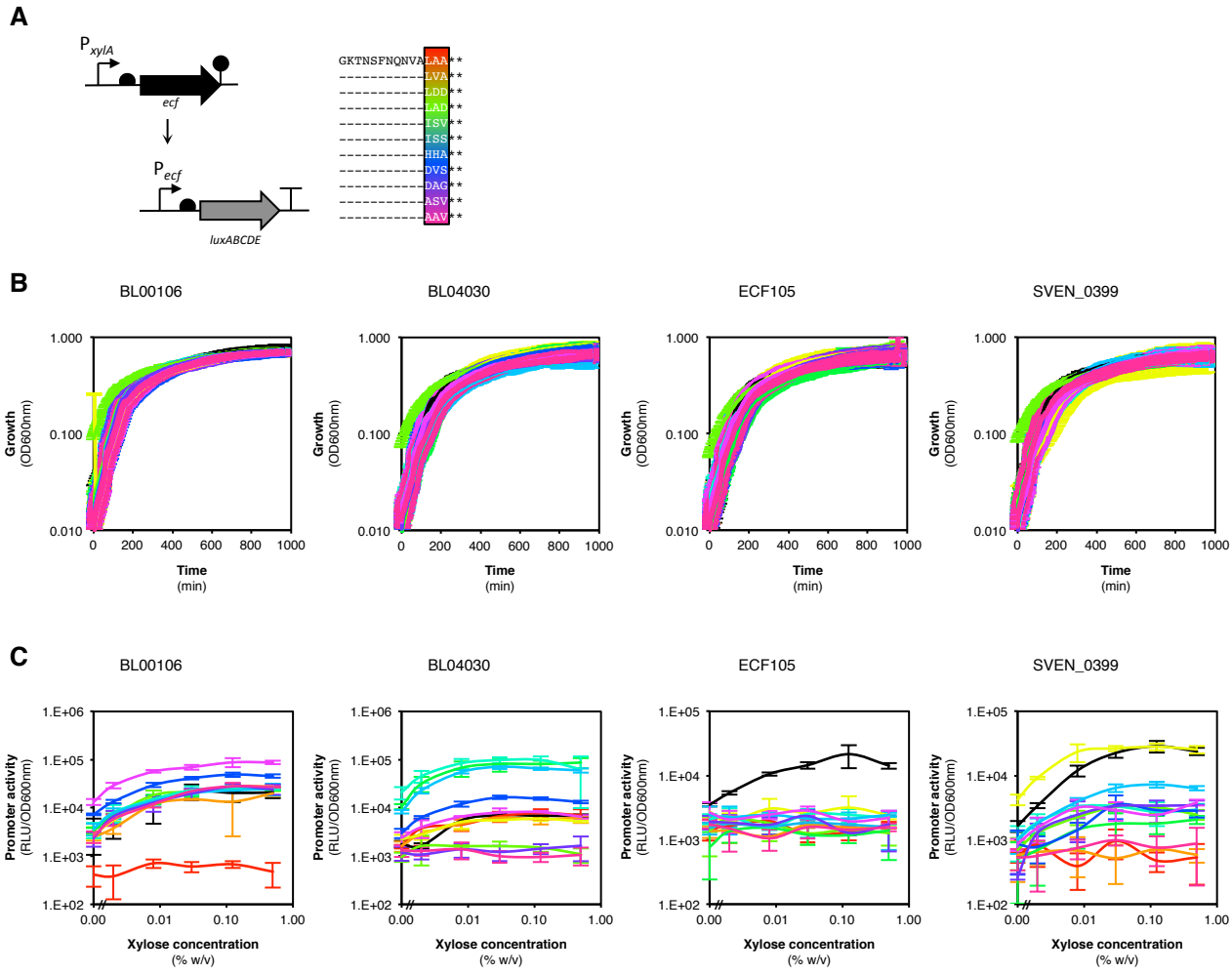

Figure S9. Behavior of the ECF switch upon addition of ssrA-tag variants, Related to Figure 2. **A.** Genetic layout of promoter-reporter constructs. Thick arrows represent open reading frames. 'T' represents terminators. Half circles represent ribosome binding sites. Thin arrows represent promoters. **B.** Growth curves of the strains containing each of the constructs represented in panel A. The inducer was added to the growing culture after 60 minutes. Final concentrations of xylose used for induction were 0, 0.002, 0.008, 0.03, 0.125 or 0.5% (w/v). Vertical bars represent standard deviations of three independent experiments. Source data can be found in Additional File 3. **C.** Dose-response curves drawn using the relative luminescence units (RLU) normalized by the optical density measured at 600 nm (OD600nm) value achieved 90 min after the addition of inducer. Final concentrations of xylose used for induction were 0, 0.002, 0.008, 0.03, 0.125 or 0.5% (w/v). Vertical bars represent standard deviations of three independent experiments. Source data can be found in Additional File 3.

VII.5 Behavior upon variation of the promoter size

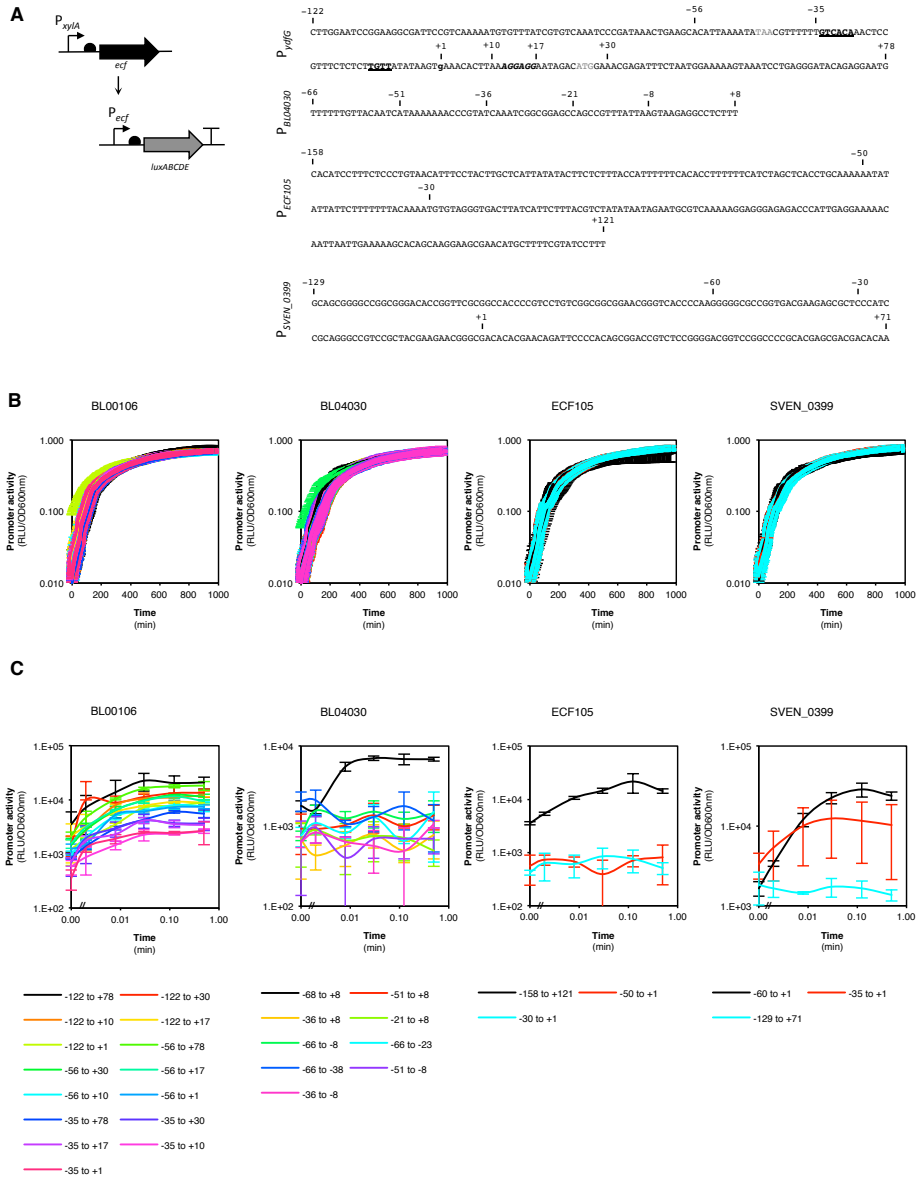

Figure S10. Behavior of the ECF switch upon variation of the promoter size, Related to Figure 2. **A.** Genetic layout of promoter-reporter constructs is depicted on the left side of the panel. Thick arrows represent open reading frames. 'T' represents terminators. Half circles represent ribosome binding sites. Thin arrows represent promoters. Promoter sequences with the relevant position numbers marked above the sequence is depicted on the right side of the panel. Stop and start codons of the neighbor open reading frames are highlighted in grey. Promoter -35 and -10 elements are underlined while +1 is marked by the use of lowercase. Ribosome binding side sequence is italicized. **B.** Growth curves of the strains containing each of the promoter variation constructs. The inducer was added to the growing culture after 60 minutes. Final concentrations of xylose used for induction were 0, 0.002, 0.008, 0.03, 0.125 or 0.5% (w/v). Vertical bars represent standard deviations of three independent experiments. Source data can be found in Additional File 3. **C.** Dose-response curves drawn using the relative luminescence units (RLU) normalized by the optical density measured at 600 nm (OD600nm) value achieved 90 min after the addition of inducer. Final concentrations of xylose used for induction were 0, 0.002, 0.008, 0.03, 0.125 or 0.5% (w/v). Vertical bars represent standard deviations of three independent experiments. Source data can be found in Additional File 3.

VII.6 Behavior under the influence of antisense transcription

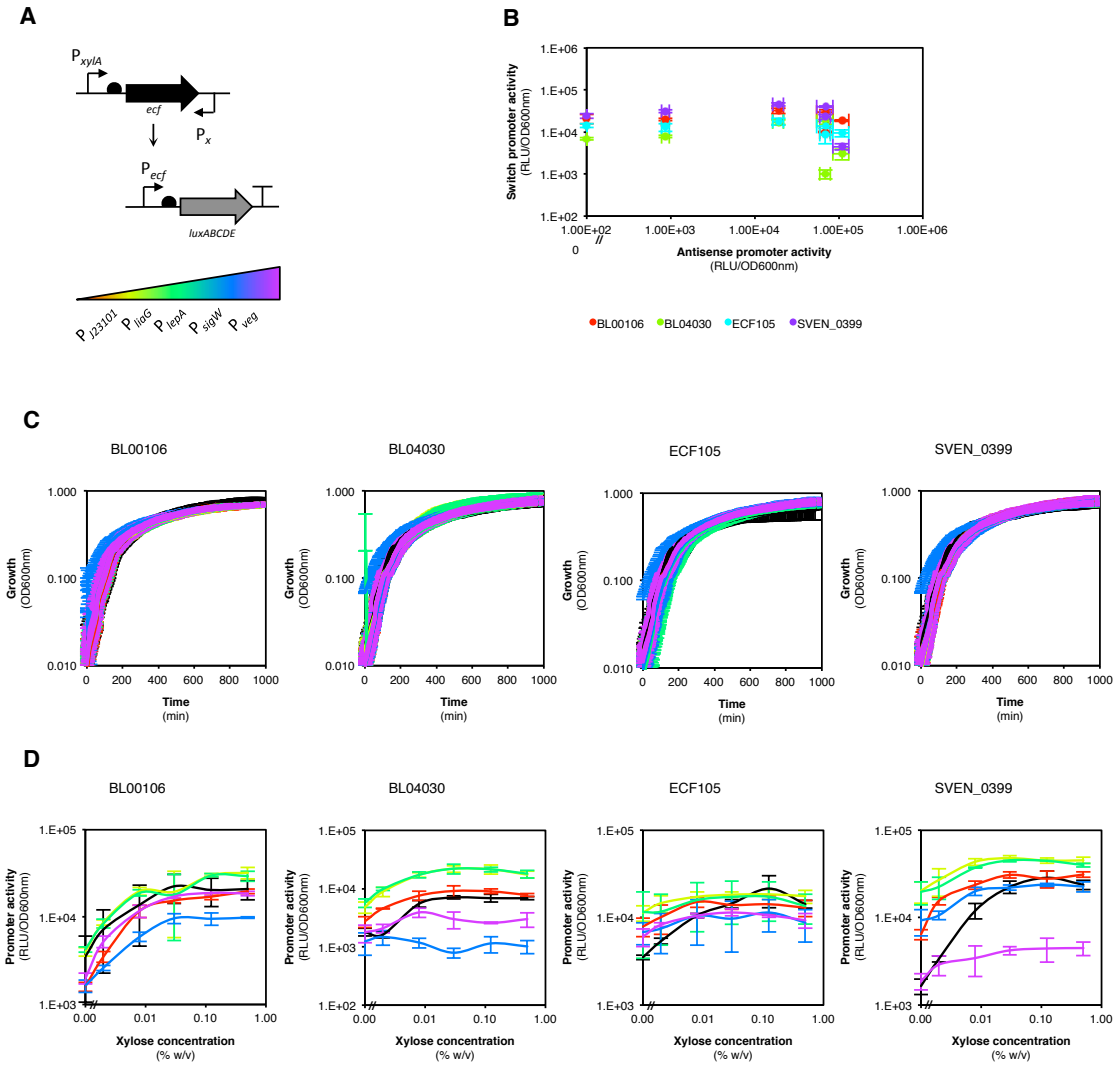

Figure S11. Behavior of the ECF switch under the influence of antisense transcription, Related to Figure 2. **A.** Genetic layout of promoter-reporter constructs is depicted. Thick arrows represent open reading frames. 'T' represents terminators. Half circles represent ribosome binding sites. Thin arrows represent promoters. The relative strength of the promoter used for antisense transcription is depicted underneath. **B.** Variation of the ECF switch activity with the activity of the antisense promoter. Data points correspond to relative luminescence units (RLU) normalized by the optical density at 600 nm (OD600nm) value 90 minutes after the addition of 0.5 % (w/v) of xylose. Vertical bars represent standard deviations of three independent experiments. Source data can be found in Additional File 3. **C.** Growth curves of the strains containing each of the ECF-promoter constructs. The inducer was added to the growing culture after 60 minutes. Final concentrations of xylose used for induction were 0, 0.002, 0.008, 0.03, 0.125 or 0.5% (w/v). Vertical bars represent standard deviations of three independent experiments. **D.** Dose-response curves drawn using the luminescence output value, represented through relative luminescence units (RLU) normalized by the optical density measured at 600 nm (OD600nm), achieved 90 min after the addition of the inducer to the exponentially growing culture. Each graph represents the measurements performed with the *B. subtilis* strain harboring the switch variants shown in panel A: without antisense promoter (black), P_{J23101} (lime), P_{liaG} (green), P_{lepA} (teal), P_{sigW} (turquoise), P_{veg} (blue). Final concentrations of xylose used for induction of P_{xylA} were 0, 0.002, 0.008, 0.03, 0.125 or 0.5 % (w/v). Vertical bars represent standard deviations calculated from three independent experiments. Source data can be found in Additional File 3.

VII.7 Robustness to the imposed modifications

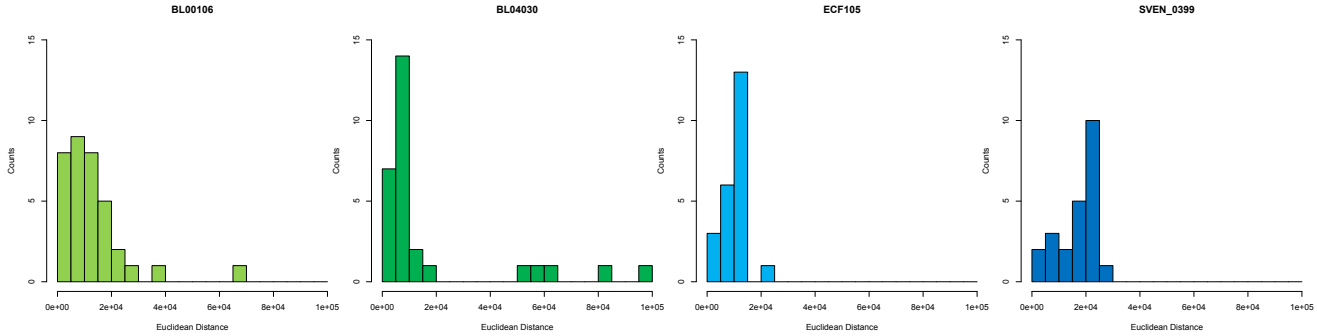

Figure S12. Distribution of Euclidean distances, Related to Figure 2. The Euclidean distance between each data point in the tridimensional scatter plots of Figure 2 and the default switch data point (black X) was calculated and their distribution plotted for each ECF switch. The Euclidean distance is a measure of the robustness of the switch to the imposed perturbation: a switch that is more robust to perturbations has a higher frequency of low distances, while a switch that is less robust to perturbations has a lower frequency of low distances.

VIII. References

Asai, K., Ishiwata, K., Matsuzaki, K., Sadaie, Y., 2008. A Viable Bacillus subtilis Strain without Functional Extracytoplasmic Function Sigma Genes. J. Bacteriol. 190, 2633–2636. doi:10.1128/JB.01859-07

Gómez-Santos, N., Pérez, J., Sánchez-Sutil, M.C., Moraleda-Muñoz, A., Muñoz-Dorado, J., 2011. CorE from Myxococcus xanthus is a copper-dependent RNA polymerase sigma factor. PLoS Genet. 7, e1002106. doi:10.1371/journal.pgen.1002106

Griffith, K.L., Grossman, A.D., 2008. Inducible protein degradation in Bacillus subtilis using heterologous peptide tags and adaptor proteins to target substrates to the protease ClpXP. Mol. Microbiol. 70, 1012–1025. doi:10.1111/j.1365-2958.2008.06467.x

Guiziou, S., Sauveplane, V., Chang, H.-J., Cler E, C., Declerck, N., Jules, M., Bonnet, J., 2016. A part toolbox to tune genetic expression in Bacillus subtilis. Nucleic Acids Res. doi:10.1093/nar/gkw624

Huang, X., Pinto, D., Fritz, G., Mascher, T., 2015. Environmental Sensing in Actinobacteria: a Comprehensive Survey on the Signaling Capacity of This Phylum. J. Bacteriol. 197, 2517–35. doi:10.1128/JB.00176-15

Jogler, C., Waldmann, J., Huang, X., Jogler, M., Glöckner, F.O., Mascher, T., Kolter, R., 2012. Identification of proteins likely to be involved in morphogenesis, cell division, and signal transduction in Planctomycetes by comparative genomics. J. Bacteriol. 194, 6419–30. doi:10.1128/JB.01325-12

Joseph, P., Fantino, J.R., Herbaud, M.L., Denizot, F., 2001. Rapid orientated cloning in a shuttle vector allowing modulated gene expression in Bacillus subtilis. FEMS Microbiol. Lett. 205, 91–97. doi:10.1016/S0378-1097(01)00449-9

Karlin, S., Mrázek, J., Campbell, A., Kaiser, D., 2001. Characterizations of highly expressed genes of four fast-growing bacteria. J. Bacteriol. 183, 5025–40. doi:10.1128/JB.183.17.5025

Pinto, D., Mascher, T., 2016. The ECF classification: a phylogenetic reflection of the regulatory diversity in the extracytoplasmic function sigma factor protein family, First Edit. ed, Stress and Environmental Regulation of Gene Expression and Adaptation in Bacteria. John Wiley & Sons, Inc.

Pinto, D., Vecchione, S., Wu, H., Mauri, M., Mascher, T., Fritz, G., 2018. Engineering orthogonal synthetic timer circuits based on extracytoplasmic function σ factors. Nucleic Acids Res. 46, 7450–7464. doi:10.1093/nar/gky614

Popp, P.F., Dotzler, M., Radeck, J., Bartels, J., Mascher, T., 2017. The Bacillus BioBrick Box 2.0: Expanding the genetic toolbox for the standardized work with Bacillus subtilis. Sci. Rep. 7, 1–13. doi:10.1038/s41598-017-15107-z

Radeck, J., Kraft, K., Bartels, J., Cikovic, T., Dürr, F., Emenegger, J., Kelterborn, S., Sauer, C., Fritz, G., Gebhard, S., Mascher, T., 2013. The Bacillus BioBrick Box: generation and evaluation of essential genetic building blocks for standardized work with Bacillus subtilis. J. Biol. Eng. 7, 29. doi:10.1186/1754-1611-7-29

Staroń, A., Sofia, H.J., Dietrich, S., Ulrich, L.E., Liesegang, H., Mascher, T., 2009. The third pillar of bacterial signal transduction: classification of the extracytoplasmic function (ECF) sigma factor protein family. Mol. Microbiol. 74, 557–81. doi:10.1111/j.1365-2958.2009.06870.x

Wecke, T., Halang, P., Staroń, A., Dufour, Y.S., Donohue, T.J., Mascher, T., Wecke, T., Halang, P., Staro, A., Mascher, T., 2012. Extracytoplasmic function σ factors of the widely distributed group ECF41 contain a fused regulatory domain. Microbiologyopen 1, 194–213. doi:10.1002/mbo3.22

Wiegert, T., Schumann, W., 2001. SsrA-mediated tagging in Bacillus subtilis. J. Bacteriol. 183, 3885–9. doi:10.1128/JB.183.13.3885-3889.2001